SUPERSWELLS

Marcia K. McNutt
Monterey Bay Aquarium Research Institute
Moss Landing, California

Abstract. Geophysicists have long sought direct, incontrovertible evidence from surface observables for convection in Earth's mantle. One of the best candidates for a phenomenon of convective origin is the South Pacific Superswell, a broad area of uplifted seafloor containing numerous volcanoes in French Polynesia. Other proposed examples of the superswell phenomenon include seafloor now located in the North Pacific that was anomalously shallow back in Cretaceous time and the present-day high topography of eastern and southern Africa. Researchers suggest that superswells form over mantle that is hotter than the global average on account of long-term absence of cooling by subducting lithosphere. Superswell mantle is melt rich, as evidenced by a fourfold increase in the rate of volcanism as compared with that of normal lithosphere. Seismic tomography suggests that the source for this diffuse, radiogenically enriched volcanism without long age progressions is a hot layer above the transition zone, rather than numerous deep-mantle plumes. Dynamic upwelling of this buoyant material in a low-viscosity zone immediately beneath the plate is responsible for both the shallow seafloor and the dip in the elevation of the Earth's sea level equipotential surface over French Polynesia. Thermal models consistent with the seismic tomography, depth, and geoid data predict extremely minor perturbations to the temperature structure in the upper 50 km of the lithosphere and thus unresolvable anomalies in both heat flow and the stiffness of the elastic plate supporting the volcanoes. Superswell volcanism is distinct from other types of volcanism by not being immediately attributable to plate separation, plate convergence, or deep-mantle plumes.

1. INTRODUCTION

Earth scientists do not doubt that the mantle convects. Simple extrapolation of surface thermal gradients into the upper mantle yields temperatures at which rocks will flow on geologic timescales when subjected to stresses of the order of 1 MPa. It has been far more difficult, however, to point to specific geologic features caused by that convection. Although plate tectonics itself is surely evidence for convection, in that the plates represent the cold, upper thermal boundary layer of a convecting system, most geologic events can be interpreted as the interactions of these plates, without requiring any knowledge of the scale or pattern of convection beneath them. The high viscosity and thermal inertia of the plates effectively shield surface geologic processes from convective forces below. For example, over the vast expanse of the ocean basins the depth of the seafloor is almost completely controlled by thermal contraction of the plates as they conductively cool, not by the viscous stresses from mantle upwellings and downwellings impinging on the base of the plates.

One exception to this rule is hotspots, which are thought to be plume-like thermal upwellings from the mantle that produce seamounts, oceanic plateaus, and broad areas of anomalously shallow topography around sites of active midplate volcanism [*Wilson*, 1963; *Morgan*, 1971]. Within the theory of plate tectonics, there is no explanation for hotspots. They do not move with the plates, but they do drift slowly with respect to each other [*Molnar and Stock*, 1987; *Acton and Gordon*, 1994; *Tarduno and Gee*, 1995; *Steinberger*, 1996]. In this paper, I make a distinction between a hotspot, which is any melting anomaly that produces more than the usual 5–7 km of igneous oceanic crust, and a plume, which is one particular explanation for a hotspot that invokes a narrow, isolated upwelling from the deep Earth. The type example of a hotspot is the Hawaiian-Emperor island and seamount chain, a line of volcanoes that erupted in the middle of the North Pacific far from any plate boundary. The age-progressive nature of the Hawaiian chain (volcanoes get monotonically older to the west and north) has led to the popularity of the plume explanation: The chain erupts as the plate drifts passively over a hot, rising plume fixed with respect to the core-mantle boundary. The fact that the plume model so successfully fits the observations from Hawaii [*Clague and Dalrymple*, 1989] has led to the general belief that all hotspots are plumes despite lack of any conclusive evidence for a deep-mantle plume beneath Hawaii or anywhere else. The scale of a hotspot is so small that only one, Iceland, has been imaged with seismic tomography [*Wolfe et al.*, 1997], and it is possible to explain anomalous depth, gravity, heat flow, and seismic velocity near hotspots as a perturbation to the thermal structure of the upper 400 km or less of the mantle [*Detrick and Crough*, 1978;

Reviews of Geophysics, 36, 2 / *May 1998*
pages 211–244
8755-1209/98/98RG-00255*$15.00*
Paper number 98RG00255

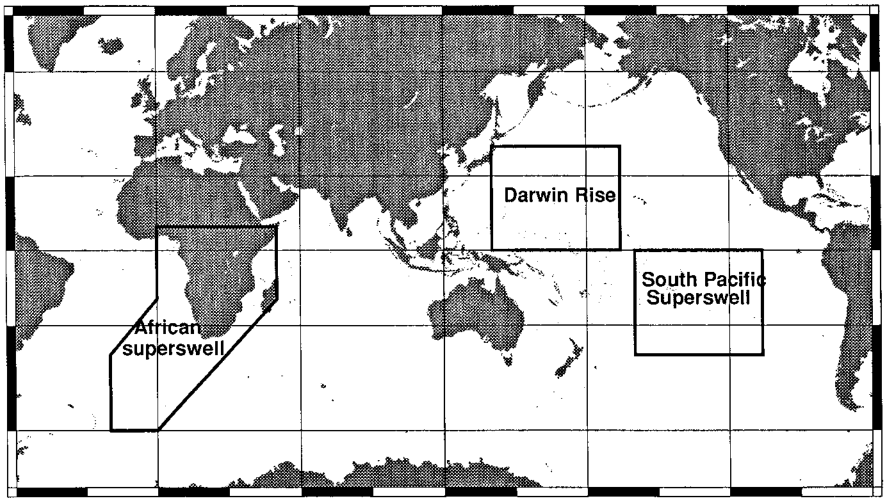

Figure 1. Locations of present-day superswells in the South Pacific and Africa and of a paleosuperswell, the Darwin Rise, in the North Pacific.

McNutt, 1987; *Wolfe et al.*, 1997]. For these reasons it has been difficult to determine whether plumes are responsible for any, some, or all hotspots; whether this type of convection transports a major or minor component of the upwelling mass and heat flux; at what depth it originates; etc.

When located away from mid-ocean ridges, a hotspot is typically surrounded at its volcanically active end by shallow seafloor less than 1000 km in cross-sectional diameter called a "swell." This swell is the direct consequence of the buoyant mantle upwelling. A "superswell" is also thought to represent a mantle upwelling, but its scale is several thousand kilometers (Figure 1). The best present-day example exists in the region of French Polynesia in the South Pacific [*McNutt and Fischer*, 1987; *McNutt and Judge*, 1990], but a similar feature existed in the Cretaceous as well [*McNutt et al.*, 1990] in an area now in the North Pacific known as the Darwin Rise [*Menard*, 1964]. Recently, the eastern and southern portions of the African plate have been proposed as a mostly continental analogue [*Nyblade and Robinson*, 1994]. Superswells are defined as anomalously high or shallow regions several thousand kilometers in extent with unusually dense concentrations of hotspots. They are large enough to be imaged by seismic tomography, and their elevation and geoid anomalies are broad enough to provide some constraints on dynamic flow beneath the plates. It is therefore timely to review the state of our understanding of the causes and consequences of superswell-type volcanism in the Pacific Ocean, whether the plume explanation is adequate, and whether the proposed continental superswell in Africa can be explained by the same simple model.

2. MENARD'S THEORY

Menard [1964] was the first to note that the height of flat-topped seamounts ("guyots") above the regional depth of the surrounding seafloor in the central and western Pacific implied that the area must have been unusually shallow when the volcanoes erupted, assuming that the flat tops were caused by erosion near sea level of former islands. He estimated that the "Darwin Rise" was ~2 km shallower than normal seafloor of the same age at the time of eruption of the seamounts. The concept of a Darwin Rise did not find much favor at that time, because it did not fit within the major tenents of plate tectonics. For example, the orientation of magnetic lineations established that the contours of the Darwin Rise did not parallel any present or paleomid-ocean ridge [*Larson et al.*, 1972; *Larson*, 1976]. *Crough* [1979] believed that the anomalous guyot depths were caused by eruption of volcanoes on the crests of more localized, elevated swells, such as that surrounding the Hawaiian hotspot. His model required discordant ages for the guyots, which thus implied that the Darwin Rise would never have existed as a single shallow feature at any one time. Dredging, dating, and drilling of the guyots have now established conclusively that the guyots are closely grouped between 80 and 120 Ma in age [*Heezen et al.*, 1973; *Winterer et al.*, 1993; *Sager et al.*, 1993; *Haggerty et al.*, 1993], thus refuting Crough's explanation.

Menard's [1964] hypothesis was later revived by *Schlanger and Premoli Silva* [1981] based on the discovery of massive basaltic sills of Cretaceous age overlying older sediments and basement in the region of the western Pacific encompassing the Darwin Rise. Synchronous volcanism over such a large region did not fit with a simple plume model. Furthermore, the sedimentary stratigraphy indicated that the basement was unusually shallow when the sills erupted. Just 2 years before his death, *Menard* [1984] reaffirmed that the Darwin Rise existed at 100 Ma in an area extending from the Magellan Seamounts to the Mid-Pacific Mountains to the Japanese Guyots (Figure 2). The lithosphere, 13–64 Myr old at the time, was 170–1600 m too shallow for its age. The

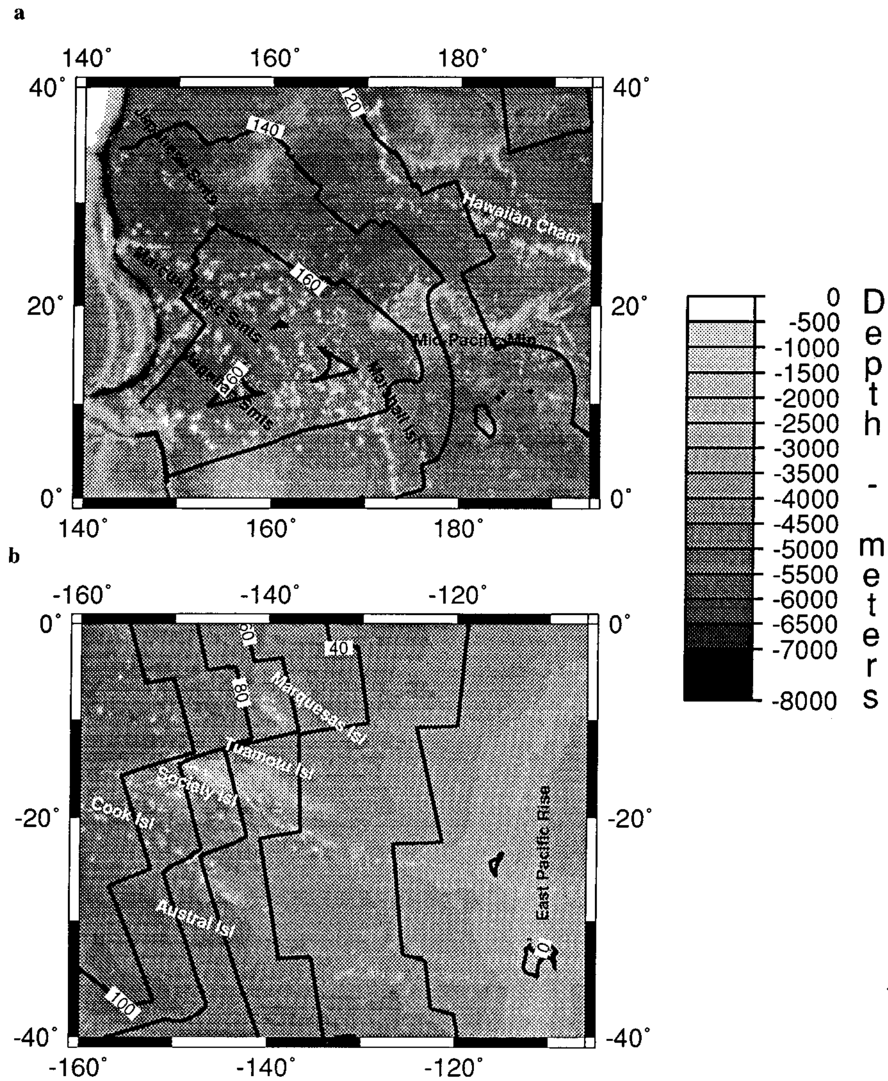

Figure 2. Bathymetry (a) of the Darwin Rise region in the North Pacific and (b) of the South Pacific Superswell region. Solid black lines show isochrons of lithospheric age [*Mueller et al.*, 1993]. The source of the bathymetric data is SYNBAPS [*Van Wykhouse*, 1973].

concentration of volcanism, he noted, was similar to that occurring in French Polynesia today. The origin of the feature still remained unclear, but Menard seemed to view it as a vast midplate swell, the collapse of which led to massive, diffuse abyssal volcanism.

The term "superswell" was first used by *McNutt and Fischer* [1987] to describe the vast area of seafloor in French Polynesia (Figure 2) that is too shallow with respect to empirical depth-age relations, overlies upper mantle with slow propagation of surface waves [*Nishimura and Forsyth*, 1985], and encompasses a large number of radiogenically enriched hotspots [*Hart*, 1984]. Furthermore, they proposed that the Darwin Rise and French Polynesia were not just similar features but that at 100 Ma the Darwin Rise was the South Pacific Superswell (hereinafter referred to as the Superswell), on the basis of plate reconstructions of *Henderson* [1985] demonstrating that the volcanoes of the Darwin Rise erupted over the same region of the mantle underlying French Polynesia today. On the basis of geophysical information available at that time they preferred to explain the Superswell as a shallow region resulting from an anomalously thin lithospheric plate, as this was the mechanism most consistent with reports of anomalously low values for the elastic strength of the lithosphere supporting the volcanoes. Furthermore, the thinned plate model was compatible with their suggestion that the Marquesas Fracture Zone, a lithospheric feature, forms the northern boundary of the superswell. In their model the concentration of volcanism was produced by easy penetration of small, ubiquitous melt bodies through a hot, thin plate.

This view that the primary cause of the superswell was a thin thermal plate was soon reversed by *McNutt and Judge* [1990] on the basis of satellite altimetry data that displayed a dip in Earth's equipotential surface over the superswell. As will be described in more detail in section 5, this observation requires a convective origin for the Superswell. Thus *McNutt and Judge* [1990] viewed convection in the mantle to be the primary cause of the superswell, with a modestly thinner thermal plate as its consequence.

In the more than 30 years since *Menard*'s [1964] original proposition, multibeam depth soundings from the Pacific, satellite altimetry data, seismic tomography, seismic reflection data, plate reconstructions, paleomagnetic paleolatitudes, and geochemical analyses of volcanic rocks have further quantified the connection between the Cretaceous Darwin Rise and the Tertiary Superswell in French Polynesia. The new data have confirmed that superswells are largely produced by mantle convection rather than by tectonic plate interactions, while pointing out the inadequacy of explaining superswells as a simple plume phenomenon.

3. CHARACTERISTICS OF SUPERSWELLS

3.1. Volcanism

One of the hallmarks of a superswell is an enhanced rate of volcanic activity, especially away from plate edges. Within the boundaries of the present-day South Pacific Superswell the Society, Cook, Austral, Tuamotu, Marquesas, and Easter island chains contribute to its anomalous volcanism. Thus 14% of the global tally of presently active hotspots [*Sleep*, 1990] is concentrated in an area representing $<5\%$ of the globe. A similar concentration of hotspots was responsible for anomalous volcanism on the Darwin Rise as well [*Henderson*, 1985; *Winterer et al*., 1993], although it has been difficult to say whether the same hotspots were active on account of uncertainties in plate reconstructions and the drift of hotspots with respect to each other [*Haggerty et al*., 1993].

Seamount production is significantly enhanced on superswell-type lithosphere. A simple way to quantify the added mass of the seamounts is to compute the difference in volume between the original (Figure 2) and median-filtered bathymetric data (Figure 3). In comparison with the original bathymetry, it is clear that the median-filtered data retain the regional depth pattern, including the midplate swells surrounding the seamount chains of Polynesia, while eliminating the effect of constructive volcanism except for the plateaus. Median filtering is far superior to smoothing via running means or low-pass filtering, both of which would simply spread the effect of localized seamounts over a broader area. The integral of the difference between the original and median-filtered maps (before the mean is subtracted from the median-filtered data) is therefore a measure of the volume contained in the seamounts. For the Darwin Rise, after the portions of the grid that contain the island arcs of the western Pacific and the Hawaiian chain are excluded, the computed volume of the seamounts is equivalent to a surface layer $h_{\text{equiv}} = 146$ m added to the Pacific plate by volcanism in the Cretaceous. By comparison, the same calculation for the identical size area in the eastern Pacific just east of the Darwin Rise (0°–40°N, 194°–248°W) yields an average of only 37 m for h_{equiv}. (For the Superswell we calculate an intermediate value that underestimates the true seamount volume on account of poor sampling; major seamount chains evident in the satellite gravity map are missing from this depth compilation [*Mammerickx*, 1992].) This calculation accounts only for the additional bathymetry produced by seamount volcanism, not the total extra mass added to the plate, in that we have not yet included the contributions from crustal thickening to compensate the seamounts, the archipelagic aprons that fill in the bathymetric moats caused by elastic flexure of the lithosphere beneath the weight of the volcanoes, or possible crustal underplating by the hotspots, all of which can be quantified with seismic data (Figure 4). However, since these masses roughly scale with that of the seamounts [*Wolfe et al*., 1994; *Filmer et al*., 1994], the same ratios of rates of superswell to nonsuperswell volcanism would hold.

Bemis and Smith's [1993] analysis of multibeam and conventional sonar records demonstrates that the excess volcanism on the Superswell is not confined to the large-scale island chains; even small seamounts are unusually numerous. Small seamounts (50–700 m in height) in the Pacific follow an exponential distribution for the decrease in numbers of seamounts with increasing size [*Smith and Jordan*, 1988]. The parameters in that distribution can be estimated for a given region using limited profiler data, and the exponential distribution can then be used to extrapolate the results over the entire region. This procedure thus avoids the problem of very incomplete bathymetric sampling in the South Pacific mentioned above. *Bemis and Smith* [1993] estimate that the number of seamounts on the superswell with height $h > H$ can be expressed as

$$v(H) = v_o \exp(-\beta H) \tag{1}$$

with $v_o = 30 \pm 3 \times 10^{-9}$ m^{-2} and $\beta^{-1} = 115 \pm 4$ m. In comparison, for a region of similar age and similar sediment thickness north of the Superswell the corresponding values are $v_o = 10 \pm 1 \times 10^{-9}$ m^{-2} and $\beta^{-1} = 75 \pm 3$ m [*Smith and Jordan*, 1988]. The derivative of v gives the change in number with change in height:

$$dv/dh = -\beta v_o \exp(-\beta h) \tag{2}$$

Conservatively assuming that the volume of a seamount is $1/3\pi r^2 h$ (most seamounts are actually flat topped rather than conical), where r is the radius of the base, and that the radius can be estimated from the height, assuming a typical 11° slope for the seamount flanks, we can then calculate the differences in volume of seamounts for superswell versus nonsuperswell lithosphere of equal areas (Figure 5). For example, the cumulative number of seamounts 200 m high or larger is 1 order of magnitude more on versus off the Superswell (Figure 5a). The absolute number of seamounts of height between 175 and 225 m on the Superswell is predicted to be ~45,000, which is 4 times more than an equivalent

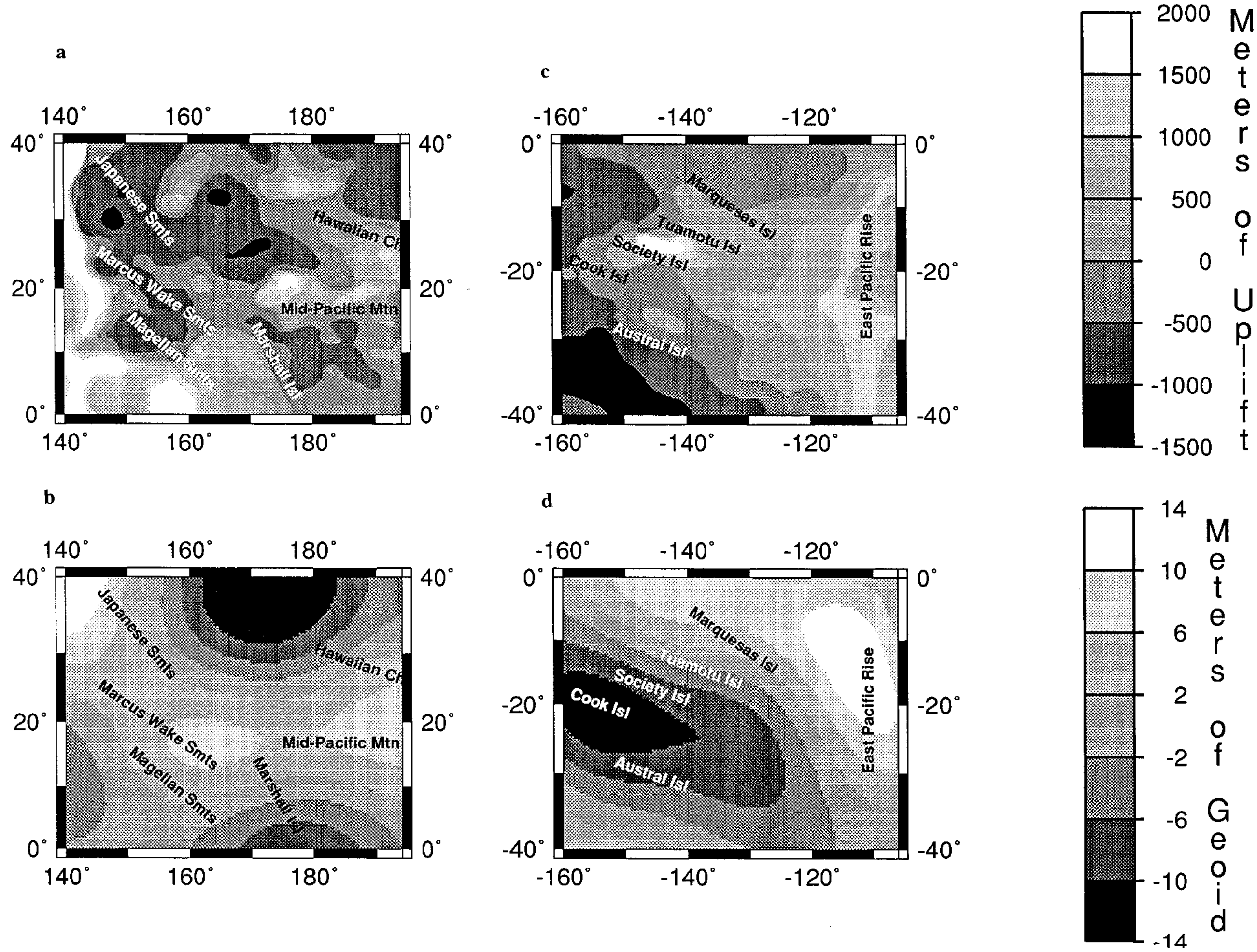

Figure 3. (a) Bathymetry for the Darwin Rise after application of a median filter [*Smith*, 1993] using the Generic Mapping Tools (GMT) [*Wessel and Smith*, 1991]. Each depth datum is replaced by the median value within a 400-km window surrounding the point. The mean depth of the entire grid has also been subtracted from the data. (b) Geoid height over the Darwin Rise in the wavelength range 3000–6000 km (spherical harmonic degrees and orders 7 through 12). (c) Median-filtered bathymetry for the South Pacific Superswell, processed in the same way as that for the Darwin Rise. (d) Geoid for the superswell at degrees 7–12.

area of seafloor off the Superswell. Taking into account the fact that seamount volume is roughly proportional to the cube of seamount height (Figure 5c), the greater number of seamounts on the Superswell results in an order of magnitude more volcanism (integral under the curves in Figure 5d).

Therefore, regardless of whether we consider number of hotspots, volume of mapped seamounts, or statistical rates of seamount volcanism, we find that the rate of volcanism on the Darwin Rise and the Superswell is 3–4 times greater than that for normal oceanic lithosphere. The style of the anomalous volcanism spans all scales, including major plateaus presumably erupted near a mid-ocean ridge, chains of midplate islands and seamounts, quasi-age-progressive volcanic ridges [*Sandwell et al.*, 1995], small lineations and abyssal flows [*Shen et al.*, 1993], and isolated seamounts.

Although the seamount distribution supports the notion that superswells are "different" than other seafloor, the cause of the fourfold enhancement in seamount production is not uniquely determined. For example, it could represent greater production of melt in a warmer or wetter asthenosphere (the weak zone beneath the lithosphere over which the plates drift), greater ease of penetration of small, ubiquitous melt bodies through a thinner and more permeable lithosphere, or some combination of the two. The fact that the anomalous volcanism extends over all scales does, however, rule out the hypothesis that a superswell is just a chance grouping of several deep-mantle plumes and leads to the question of whether the Polynesian hotspots such as Society and Macdonald are deep-mantle plumes or whether they are just the upper end-member of a continuum in volumes of melt production.

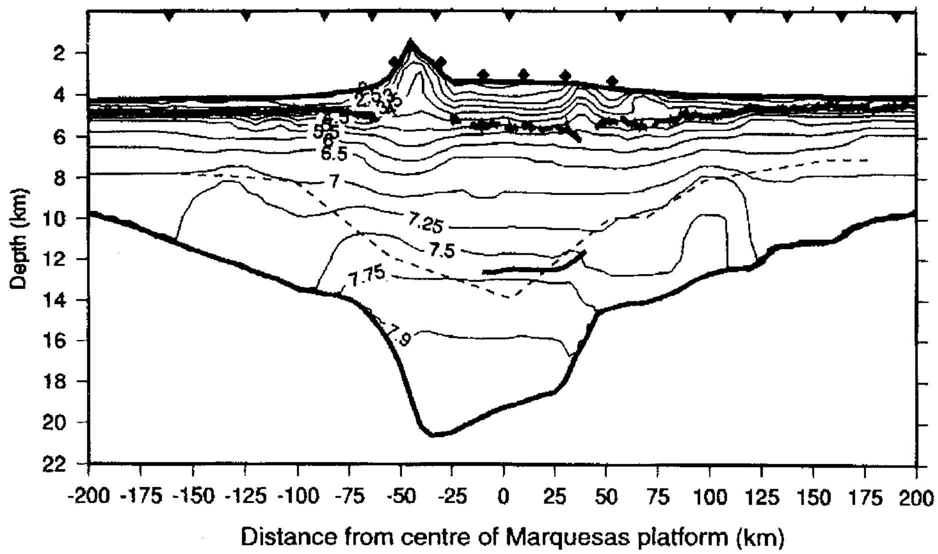

Figure 4. Seismic velocity model for a cross section of the Marquesas Islands derived from ocean bottom seismometer (diamonds) and sonobuoy (inverted triangle) refraction records. The locations of the seafloor, the top of the preexisting crust, the relict Moho, and the current Moho (bold curves) are overlain on the velocity contours (km s^{-1}). The approximate depth of the deepest turning *P* wave is shown as a dashed line. Velocities below this are based on a simple extrapolation of gradients. The material above the boundary of the preexisting crust is largely extrusive volcanic rocks, but an equal volume of intrusive plutonic rocks has been emplaced between the relict and present Moho. From *Caress et al.* [1995]; copyright 1995 Macmillan Magazines Ltd.

3.2. Depth-Age Relations

A second distinctive feature of a superswell, and the source of the name, is shallow seafloor compared with the average depth for that age extending over thousands of kilometers. Recently, the very existence of anomalously shallow depths for the South Pacific Superswell has been challenged by *Levitt and Sandwell* [1996]. They suggested that the entire depth anomaly in the South Pacific is an artifact of faulty gridding and contouring of ship soundings in creating the digital database of Figure 2. Subsequent studies using more extensive data sets have put to rest this "bad data" hypothesis [*McNutt et al.*, 1996; L. Sichoix et al., Analysis of modal depths from single and multibeam bathymetry and reexamination of the swells and the Superswell in the South Pacific, submitted to *Journal of Geophysical Research*, 1997 (hereinafter referred to as Sichoix et al., submitted manuscript, 1977). Using a newly compiled data base of >400,000 ship soundings from oceanographic expeditions and the French Navy, all carefully examined for quality control [*Sichoix and Bonneville*, 1996], these studies demonstrate close agreement between modes (i.e., the most common values) of depth as a function of age calculated from the original ship soundings and those derived from the gridded database. Even after removing data from the vicinity of the Polynesian hotspot chains (Figure 6), modal depths (Sichoix et al., submitted manuscript, 1997) are ~1 km shallower than predicted by the half-space model that provides a reasonable fit to <70 Ma lithosphere elsewhere in the world's oceans [*Parsons and Sclater*, 1977; *Carlson and Johnson*, 1994]. The depths are anomalously shallow even in comparison with models with very thin thermal plates, such as that of *Stein and Stein* [1992]. The shallow depths are a real phenomenon that cannot be explained as the superposition of local hotspot effects. In fact, of the 32 tectonic regions on the flanks of mid-ocean ridges analyzed by *Marty and Cazenave* [1989], no region deepens more slowly away from the mid-ocean ridge than does the Superswell. This region of slow subsidence extends all the way east to the East Pacific Rise (EPR) but not across it [*Cochran*, 1986]. The depth anomaly diminishes in amplitude north and south of the Marquesas and Austral Fracture Zones, respectively, but these lithospheric features do not strictly bound it (Sichoix et al., submitted manuscript, 1997).

It is difficult to attribute the anomalous subsidence of the Superswell solely to conductive cooling of the lithosphere. The predicted rate of subsidence, w, for seafloor overlying a cooling half-space is

$$w = \frac{\rho_m}{\rho_m - \rho_w} \frac{T_m \alpha}{\pi} (4\pi\kappa t)^{1/2} \tag{3}$$

in which ρ_m and ρ_w are the densities of mantle and water, respectively, T_m is the temperature at the mid-ocean ridge, α is the coefficient of thermal expansion, κ is the thermal diffusivity, and t is lithospheric age. According to this expression, merely making the asthenosphere beneath the mid-ocean ridge hotter should increase the subsidence rate, not decrease it. In several areas of the ocean basins, the fact that the seafloor older

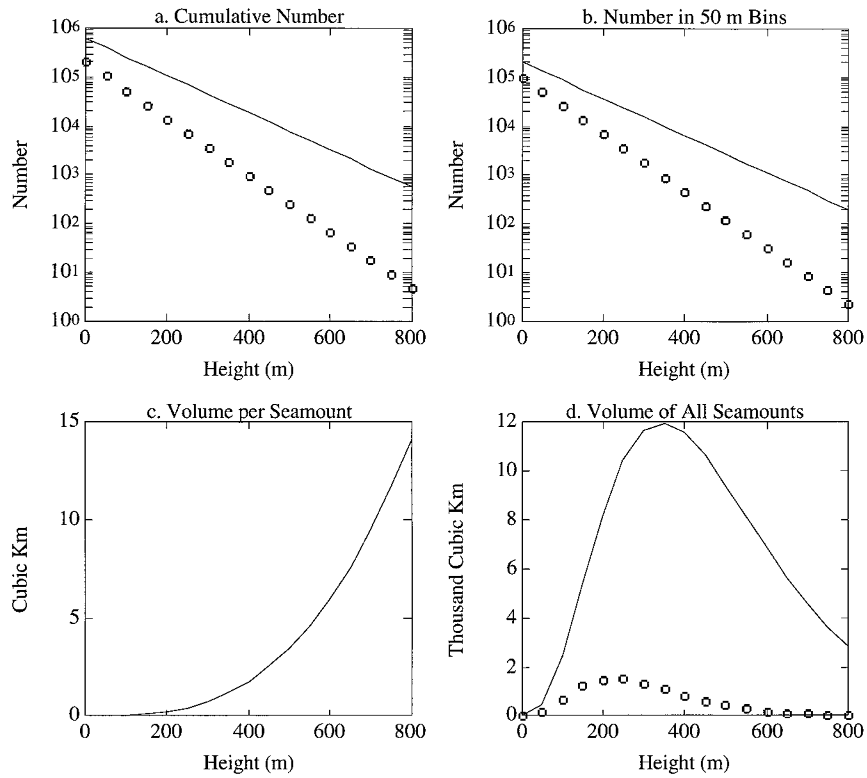

Figure 5. Statistical distribution of seamounts 50–700 m in height on the South Pacific Superswell (solid line) and just north of the Superswell (open circles) using parameters determined by *Bemis and Smith* [1993]. (a) Cumulative number of seamounts (vertical axis) with height greater than the value given on the horizontal axis. (b) Absolute number of seamounts in height ranges ±25 m. (c) Theoretical relationship between volcano height and volume assuming conical shape and 11° slope. (d) Distribution of seamount volumes in ±25-m height ranges. The integral between the two curves represents the excess volcanism on the Superswell contributed by small seamounts.

than 70 Ma is too shallow with respect to the half-space cooling relation has been attributed to the effect of a lower boundary on cooling of the lithosphere; that is, it cools as a plate rather than a half-space [*Parsons and Sclater*, 1977; *Stein and Stein*, 1992]. In the case of the Superswell, *McNutt and Fischer* [1987] originally explained the shallow depth for 40–80 Ma lithosphere as cooling of a thermal plate no more than 75 km thick, but then the subsidence rate is actually too slow to fit the depth of seafloor older than 80 Ma well. Clearly, something more complicated than cooling of a thermal plate or half-space is contributing to the anomalous subsidence in French Polynesia.

Regardless of the cause of the slow subsidence for the Superswell, the same conditions apparently existed when the Darwin Rise was volcanically active at 100 Ma. Its paleodepth as a function of lithospheric age closely resembles that of the present Superswell (Figure 7), based on analysis of the height of the wave-eroded volcanic rocks at guyot summits above the surrounding seafloor in the Japanese, Wake, and Mid-Pacific seamounts [*McNutt et al.*, 1990]. The interpretation of this paleodepth information in terms of a reduced subsidence rate of abnormally shallow seafloor at the time of volcanism has been confirmed by ocean drilling of the reef caps of Darwin Rise guyots [*Larson et al.*, 1995].

Several studies have attempted to use the depths of the Darwin Rise lithosphere today to constrain the origin of superswells. Unfortunately, the answer depends on the choice of reference level (the depth assumed for "normal" seafloor). For example, *Davies and Pribac* [1993] have argued that there is no plausible physical explanation for why thermal subsidence of the seafloor should depart from the predictions of the half-space model. With this model as the reference, they find depth anomalies of 1 km for the Darwin Rise today, which they attribute to convective uplift. If one assumes a plate model for the lithosphere, depending on the thickness of the plate, the present-day depth anomaly is either small (125-km-thick plate [*McNutt et al.*, 1990]) or nonexistent (95-km-thick plate [*Stein and Stein*, 1994]). However, *Marty and Cazenave* [1989] found that there are only two other regions in the world's oceans out of the 32 regions they surveyed where old ocean floor "flattens" as predicted by the plate model (and these two regions contain the Bermuda and Cape Verde hotspots). Therefore it is questionable whether the Darwin Rise even today is evolving like normal seafloor [*Davies and Pribac*, 1993].

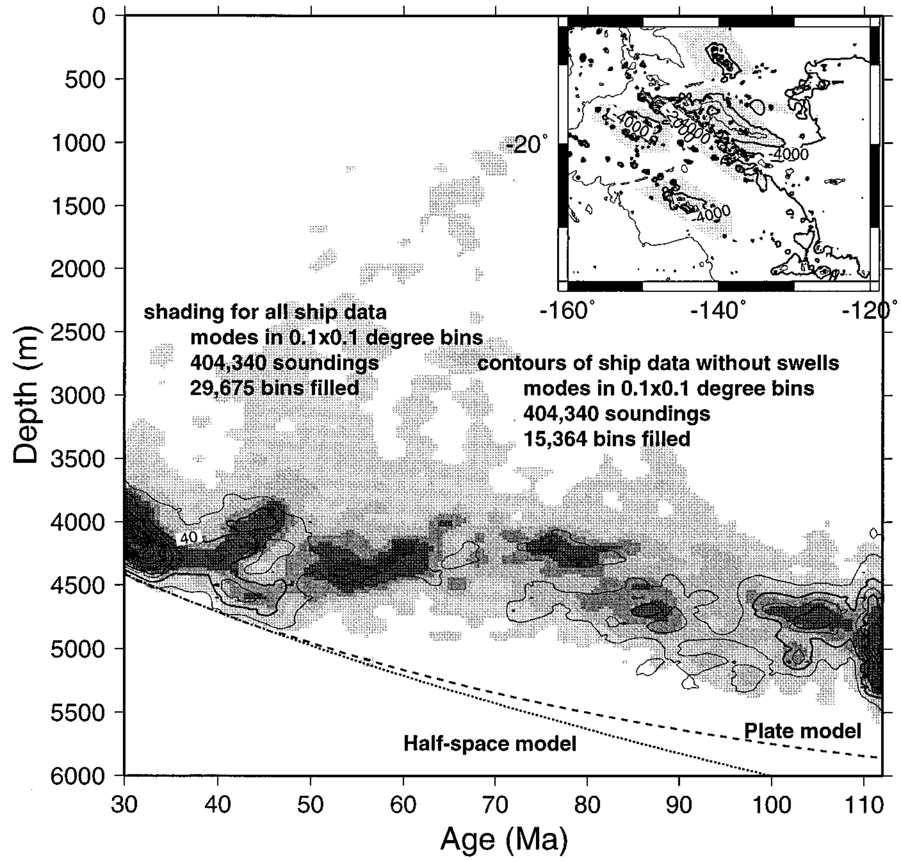

Figure 6. Contours of the modes of depths from ship soundings in the South Pacific plotted as a function of lithospheric age. The soundings were sorted into $0.1° \times 0.1°$ latitude-longitude bins prior to calculating the mode so that frequently sampled bins would not have undue influence on the result. Less than 10% of the possible bins in French Polynesia are actually sampled. Regions around each of the major hotspot chains, as shown in the inset, were also avoided in order to sample the depth-age relation away from the influence of hotspots. For comparison, theoretical subsidence curves for the half-space (small dots) and plate (dashes) cooling models are shown for reference. From Sichoix et al. (submitted manuscript, 1997).

In fact, if one excludes data from the vicinity of the Darwin Rise, the Bermuda Rise, and the Cape Verde Rise (all affected by hotspots), other areas with old seafloor show no flattening of depth as a function of age. *Smith and Sandwell* [1997] argue that the distribution of area of seafloor as a function of depth in the oceans requires that the thickness of the lithosphere exceed 150 km. For plates thinner than 150 km the asymptotic depth for old seafloor is reached at ages well younger than the oldest surviving seafloor and should produce a strong peak in the distribution that is not observed. However, until some consensus is reached as to what the depth of old (>90 Ma) seafloor should be and why it departs from that of the half-space model (if it does), it is difficult to bound the old-age behavior of superswells.

One aspect worth addressing is the extent to which the shallow depths might not be a thermal or convective phenomenon. Depth can also be reduced by thickening the crust, adding sediment to the top of the plate, or altering mantle mineralogy to less dense rock forms. Clearly, the crust has been thickened locally beneath the plateaus, islands, and seamounts, but this effect cannot explain the shallow depth modes in Figure 6 away from the major volcanic chains. Furthermore, multichannel seismic reflection data, such as those shown in Figure 8 from a line shot between the Tuamotu and Society Islands, image a perfectly normal thickness for the crust (2 s of two-way travel time, or ~6 km of crust) and only a thin veneer of sediment. For comparison, to produce a 1-km depth anomaly on lithosphere 70 Myr old (about what is seen in Figure 6), the crust along this line would have to be 9.5 km thick, taking into account isostatic compensation for the thickened crust. Similar multichannel seismic data are available for the Marquesas [*Wolfe et al.*, 1994; *Caress et al.*, 1995] and Austral [*Jordahl et al.*, 1995] chains as well and show no anomalous thickening of the crust. Although no sediment corrections have been applied to the data in Figure 6, sediment thicknesses are typically a few hundred meters in the central Pacific, such that after correction for isostatic loading, their effect is negligible. Indeed, the best fitting regression line to the data from the Superswell region (Figure 6) is identical to that determined by *Marty and Cazenave* [1989] using sediment-corrected data and indicates a rate of subsidence (214 ± 40 m $Myr^{-1/2}$) that is only 60% of that determined by *Parsons and Sclater* [1977] (350 m $Myr^{-1/2}$) from fits to data from the North Pacific and North Atlantic.

Jordan [1979] has suggested that the extraction of basaltic melt at depth by a hotspot should leave behind a buoyant layer (on account of the preferential extration of Fe over Mg and removal of Al and other elements that would form the dense mineral garnet) that might contribute to the elevation of midplate swells. *Phipps Morgan et al.* [1995] suggest that this layer depleted in basaltic constituents would eventually thin and spread, causing subsidence of a hotspot swell and overall reduction in the subsidence rate of the surrounding seafloor. The height of a column of depleted material h_d produced by basalt extraction is

$$h_d = h_b/f \tag{4}$$

where h_b is the volume per unit area of basalt produced and f is the mean fraction of melt from the source region. The reduction in density of the residuum is given by

$$\Delta\rho = \rho_m \beta f \tag{5}$$

in which ρ_m is the density of undepleted mantle and β is the chemical depletion factor, which they assume to be 0.06. In calculating the integrated buoyancy in a crustal column due to melt extraction, $\Delta\rho\ h_d$, the f factors cancel out. As is shown schematically in Figure 9, the average amount of basalt per unit area contributing to topography on superswell-type lithosphere, h_{equiv}, is only 150 m, but this number must be multiplied by a factor of 6 to add in the basaltic material in the flexural moat compensating the load [*Wolfe et al.*, 1994; *Filmer et al.*, 1994], and the total must be doubled again in cases where magma underplates the crust [*Caress et al.*, 1995]. For the Darwin Rise a layer of topography 150 m high is associated with as much as 1.8 km of crustal thickening and production of an integrated column buoyancy through basalt extraction of 360,000 kg m^{-2}. Dividing this last number by the effective density of seafloor topography (density of basalt − density of water) yields only ~200 m of seafloor shallowing. This could be a significant contribution (~20%) to depth anomalies with respect to the half-space cooling model over the Darwin Rise but is not the entire explanation.

3.3. Radiometric Ages

One of the more curious features of superswell-type volcanism is the lack of long-term age progression in the volcanic chains, as would be predicted if they were caused by drift of the plate over deep-mantle plumes. Unlike the case for the Hawaii-Emperor chain, consistent age progressions along any one chain in both the South Pacific Superswell and the Darwin Rise are of the order of 10 Myr or less. For example, in the Marquesas Islands the age progression extends only from 6 to 1 Ma [*Duncan and McDougall*, 1974], the rate is too slow to be consistent with motion of the Pacific plate over a fixed plume [*Desonie et al.*, 1993], and the orientation of the chain is too northerly to align with the direction of absolute plate motion as determined from the azimuth of the Hawaiian chain. Society ages range only from 0 to 4.3 Ma [*Duncan and McDougall*, 1974], and the Geosat gravity map shows a line of volcanoes extending hundreds of kilometers to the southeast of "zero age," exactly the opposite direction of absolute plate motion.

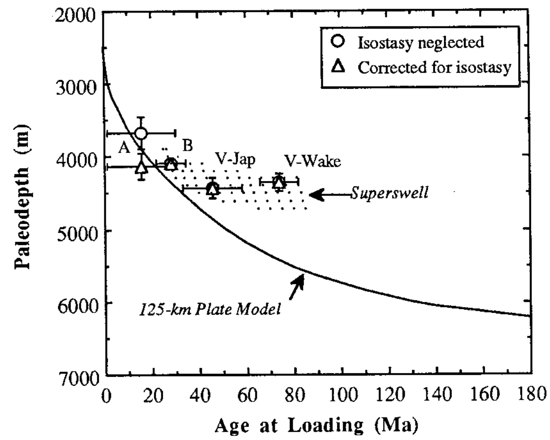

Figure 7. Paleodepth versus age of the lithosphere at the time of loading for the guyots of the Darwin Rise. At the time they drowned the "A"-type guyots were atolls (principally in the Mid-Pacific Mountains), the "B" type were islands surrounded by barrier reefs (principally in the Japanese Seamounts), and the "V" type were volcanoes without reefs (principally in the Japanese and Wake seamounts). Error bars on the paleodepth reflect the scatter in the population of all guyots with that classification. Error bars on the age reflect scatter in the population as well as uncertainty in the age of lithosphere at the time of volcanism. The dotted region shows the present-day depth-age distribution for the South Pacific Superswell. From *McNutt et al.* [1990].

The Pukapuka volcanic ridge system [*Sandwell et al.*, 1995], which trends across the Superswell from 18°S, 117°W, to 15°S, 140°W, may be typical of superswell-type linear volcanism. Volcanism occurs as a series of en echelon ridges built of coalesced cones with radiometric dates between 5.6 and 27.5 Ma. While the age of volcanism, in general, decreases to the southeast, samples separated by a distance of 2000 km differ in age by only 5 Myr, less than one-third the age range that would be predicted from drift over a fixed plume (Figure 10). In the Cook chain the radiometric dates give the impression of rapid migration of volcanism both to the northwest and to the southeast from Rimatara, beginning at ~25 Ma (Figure 10). In the southern Australs, there are two separate but almost completely superimposed periods of linear volcanism [*McNutt et al.*, 1997], the first at ~30 Ma and the second within the past few million years (Figure 10).

The radiometric dates from numerous dredging and drilling expeditions to the Darwin Rise cannot be interpreted in terms of migration of the plate across a few

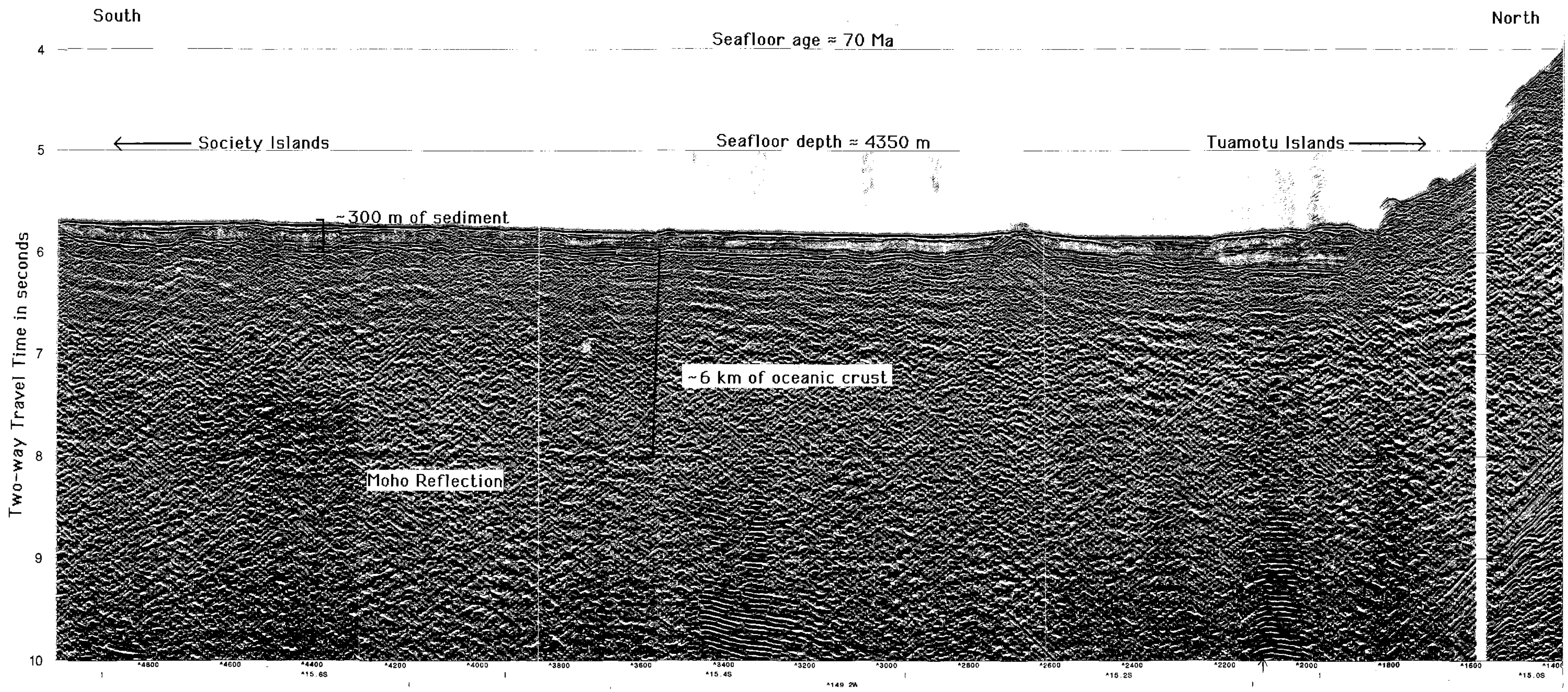

Figure 8. Multichannel seismic cross section between the Society Islands and the Tuamotu Islands. These data were acquired along the northern 1/3 of the cruise track plotted in Figure 12a during expedition EW9103 of the *Maurice Ewing*. The seismic section shows ~300 m or less of nearly transparent pelagic ooze overlying the volcanic basement. The Moho reflection at ~8 s yields a volcanic crustal section ~2 s (6 km) thick. Even after correction for the pelagic ooze, the seafloor here is ~1 km shallower than similar-aged lithosphere elsewhere in the world's oceans, and the difference is not attributable to excess crustal thickness.

fixed plumes either. One difficulty for the Darwin Rise is that the absolute plate motion direction is poorly known before ~95 Ma, especially independently of the trends of Darwin Rise seamount chains. Like the Superswell, the volcanism occurs as a number of intersecting and crosscutting chains with different orientations and little consistent progression in age from one edifice to the next [*Winterer et al.*, 1993].

In both regions the lithosphere exerts a considerable influence on the exact location and volume of volcanism.

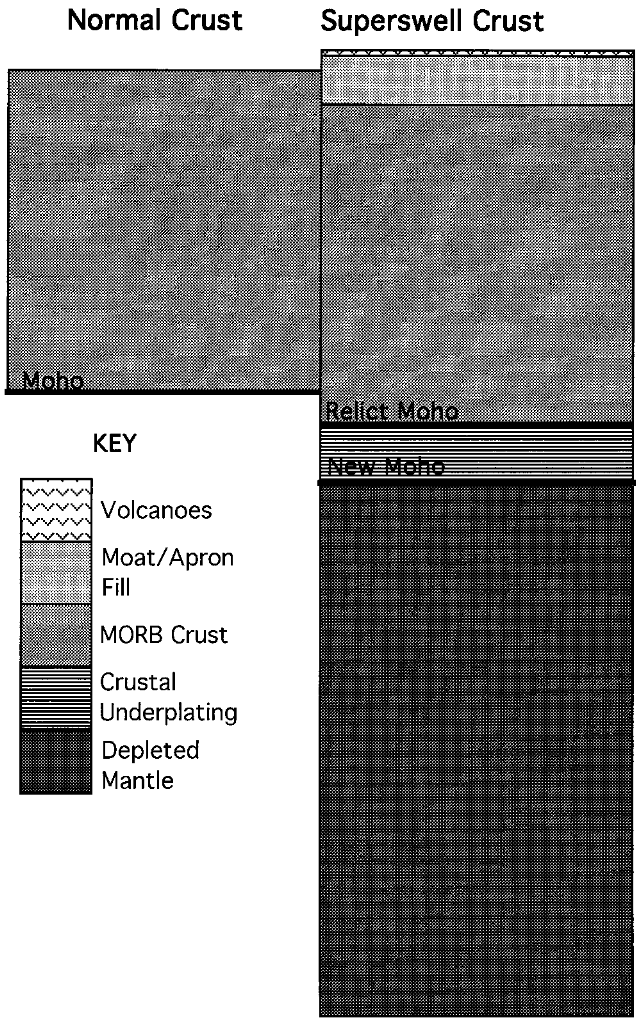

Figure 9. Representative "averaged" columns for normal versus superswell crust if the effects of anomalous volcanism were distributed evenly over all affected seafloor. The thickness of the "volcanoes" layer is calculated from bathymetric maps. The thickness of the moat/apron fill and crustal underplating is estimated from seismic data such as those in Figure 4. The amount of extra mantle that would be depleted in its basaltic constituents by excess superswell volcanism is computed assuming that the mean fraction of melt f, is 20%. Since this is likely an upper bound, the thickness of the depleted layer is a minimum. The net effect on regional depth from these volcanic/chemical effects is about 200 m, except in the immediate vicinity of the volcanoes, where the height of the edifice must be included.

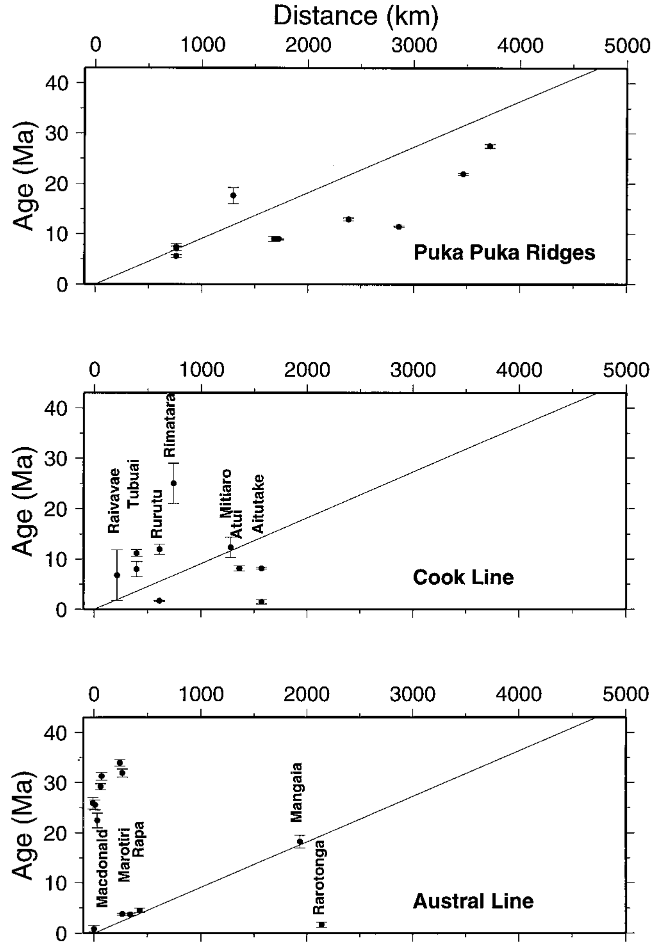

Figure 10. Radiometric ages of volcanoes as a function of distance from a hotspot for several lineations on the South Pacific Superswell. For the Austral Islands the location of zero age is the presently active Macdonald Seamount. For the Cook Islands and the Pukapuka Ridges the location of zero age is conjectural. Error bars for the Pukapuka Ridges are the analytical uncertainty of Ar-Ar dates from dredged basalt samples [*Sandwell et al.*, 1995]. The error bars for the Cook and Austral Islands are age ranges based on multiple determinations of K-Ar geochronology [*Barsczus*, 1980; *Dalrymple et al.*, 1975; *Duncan and MacDougall*, 1976; *Turner and Jarrard*, 1982] and from Ar-Ar geochronology [*McNutt et al.*, 1997]. The diagonal lines show the predicted age-distance relationship for motion of the Pacific plate over a fixed mantle plume at a rate of 110 km Myr^{-1}.

This aspect is most easily seen in Geosat and ERS-1 altimetric images of the gravity field (Plate 1), which show that the outlines of plateaus such as the Mid-Pacific Mountains and the Tuamotu follow lithospheric cracks such as ridges, transforms, and propagating rifts [*Ito et al.*, 1995]. Many hotspot traces appear to begin or end, or at least undergo a rapid change in volume output, at fracture zones [*McNutt et al.*, 1989]. In the southern Austral Islands, younger volcanoes frequently erupt on the flexural arches of older edifices [*McNutt et al.*, 1997].

If the ages of the volcanoes on the Superswell are

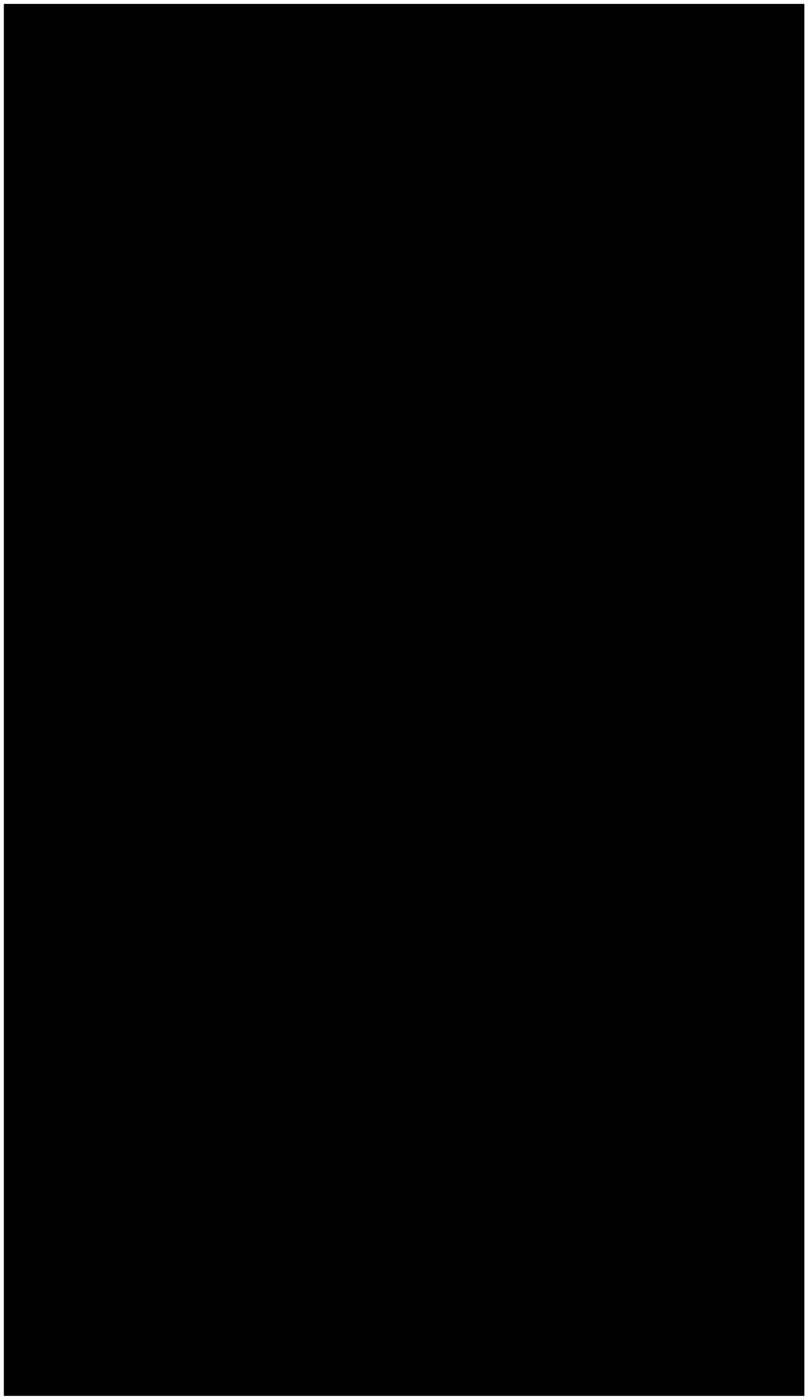

Plate 1. Shaded relief maps of the gravity field over the (a) Darwin Rise and (b) the South Pacific Superswell derived from Geosat and ERS-1 satellite altimetry. Illumination is from the northwest. Data are courtesy of W. Smith and D. Sandwell (1995).

used to estimate how long thermally anomalous conditions might have existed in this region, then we would assign an age of at least 35 Ma, equivalent to the age of the oldest volcanoes in the Australs [*McNutt et al.*, 1997]. How much longer this superswell will remain active is impossible to assess. Active volcanism is still occurring at Macdonald Seamount in the Austral chain [*Norris and Johnson*, 1969; *Talandier and Okal*, 1984a], Adams Seamount 80 km southeast of Pitcairn Island [*Stouffers et al.*, 1990], and several islands and seamounts at the southeast end of the Society Islands, including Mehetia and Tehitia [*Talandier and Okal*, 1984b, 1987]. A small seamount dredged southeast of the Marquesas Islands yielded an Ar-Ar date of 100,000 years (age determined by R. Duncan and reported by *Jordahl et al.* [1995]).

Again on the basis of the ages of sampled volcanoes, the Darwin Rise was apparently active from before 120 Ma to ~85 Ma, a period of at least 35 Myr. One possible interpretation of these age dates is that the Darwin Rise and the Superswell are separate "pulses" of anomalous volcanic activity separated by ~45 Myr [*McNutt and Fischer*, 1987]. The other possibility is that the Superswell is but the last gasp of a major Cretaceous thermal event that created the Darwin Rise [*Larson*, 1991a]. There are some seamounts, such as parts of the Line Islands [*Schlanger et al.*, 1984; *Epp*, 1984], that erupted between 85 and 40 Ma, but volumetrically, they are not as significant as the mid-Cretaceous and late-Tertiary volcanism.

3.4. Potential Field Anomalies

Perhaps the most unexpected feature of the South Pacific Superswell is the large dip in the Earth's geoid over its center (Figure 3) [*McNutt and Judge*, 1990]. The geoid represents the height of Earth's sea level equipotential surface. Uplifted seafloor, per se, represents a mass excess at the Earth's surface that increases the equipotential and results in a geoid high. All mechanisms of isostatic compensation for uplifted seafloor involve some sort of reduction of density at depth to offset the mass excess of the shallow seafloor. Many common isostatic mechanisms, such as crustal thickening or lithospheric reheating, result in mass dipoles: a surface mass excess overlying a subsurface mass deficit of equal magnitude. Because the mass excess is closer to Earth's surface, the net effect is to increase the geoid height immediately over the dipole, with the size of the high increasing with the offset between the uplifted seafloor and its buried compensation. For example, the more localized midplate swells are indeed characterized by geoid highs [*Crough*, 1978], with the magnitude of the high indicating a dipole separation (compensation depth) of ~60 km [*McNutt and Shure*, 1986].

As was argued by *McNutt and Judge* [1990], the negative anomaly over the Superswell is absolutely inconsistent with any dipole mechanisms of compensation and points to dynamic support from convection in a low-viscosity zone directly beneath the plate. Dynamic compensation can be thought of as a mass tripole: The mass excess or deficit of a downwelling or upwelling, respectively, is approximately compensated by the warping it produces on any density discontinuities in Earth to which it is viscously coupled, such as the surface and the core-mantle boundary. Earth's viscosity structure influences the amount of viscous coupling. If a low-viscosity zone lies between an upwelling mass and Earth's surface, then the rising mass will be relatively inefficient at warping the surface and will rather be largely compensated from below through deformation of deeper density discontinuities. This is exactly the scenario envisioned by *McNutt and Judge* [1990]: The density tripole consists of a broad, low-density upwelling in the upper mantle compensated by uplift of both the surface and the core-mantle boundary. The positive geoid anomaly from the core-mantle boundary is so broad after upward continuation through the entire mantle that it is undetected at wavelengths corresponding to the size of the Superswell. Although the surface uplift is shallower than the mantle upwelling, because it compensates only a part of the mass deficit, its effect on the geoid is much less, leading to a net geoid low over the Superswell.

The geoid over the Darwin Rise today (Figure 3) shows neither this same strong, inverse correlation between geoid and topography nor a pronounced geoid low over the Cretaceous island and seamount chains. Unfortunately, we have no way to determine what the geoid was over the Darwin Rise when it was volcanically active. If the geoid when the Darwin Rise was active did resemble that of the Superswell today, then there should have been nearly a 40-m rise in sea level in the past 100 Myr based on examining the total difference in geoid elevation between the South and North Pacific (degrees 2–12). Separating this "dynamic" drop in sea level from other, much larger global and regional effects (caused by, for example, changes in the global volume of the oceans or regional thermal subsidence of the seafloor) is nearly impossible, especially since four out of the six carbonate caps on the summits of Darwin Rise guyots that have been sampled by drilling died rather mysteriously between 100 and 110 Ma [*Larson et al.*, 1995], leaving no record of any subsequent sea level changes.

Superimposed on the long-wavelength geoid low over the Superswell are shorter-wavelength (<1000 km) geoid highs associated with the swells underlying the major island chains, although the size of the swells in both the geoid and the bathymetry is much smaller on the Superswell as compared with data from the Hawaiian swell. The size of the Hawaiian geoid anomaly as compared with the height of the swell yields a compensation depth of 70 ± 10 km, suggesting that heat from the Hawaiian plume has penetrated only into the lowermost part of the lithosphere [*Crough*, 1978; *McNutt and Shure*, 1986]. A similar analysis of the geoid over the Marquesas swell yields a compensation depth of only 45 ± 5 km [*Fischer et al.*, 1986], but there is a large age difference. The Marquesas Islands lie on only 50–60 Ma lithosphere [*Kruse*, 1988], whereas the Hawaiian lithosphere is ~90 Ma.

Figure 11 shows the geoid and bathymetry for the Society swell, which at 70 Ma is closer to the Hawaiian example in the age of the seafloor. After subtracting the long-wavelength geoid low that encompasses all of French Polynesia the geoid anomaly (with the effect of the volcanoes and their compensation removed) is nearly 1000 km across, a few meters in amplitude, and elongated in the direction of absolute plate motion. If we assume that this geoid anomaly has a deep compensation depth, such as 70 km, only a small topographic swell of 220 m is required for the sum of the geoid high from the topography and the geoid low from the compensation to equal the observed signal. Assuming a shallow compensation depth of 30 km requires a much larger topographic swell, 800 m, to produce the observed net geoid because the excess mass of the topography and the mass deficit from its compensation more nearly cancel

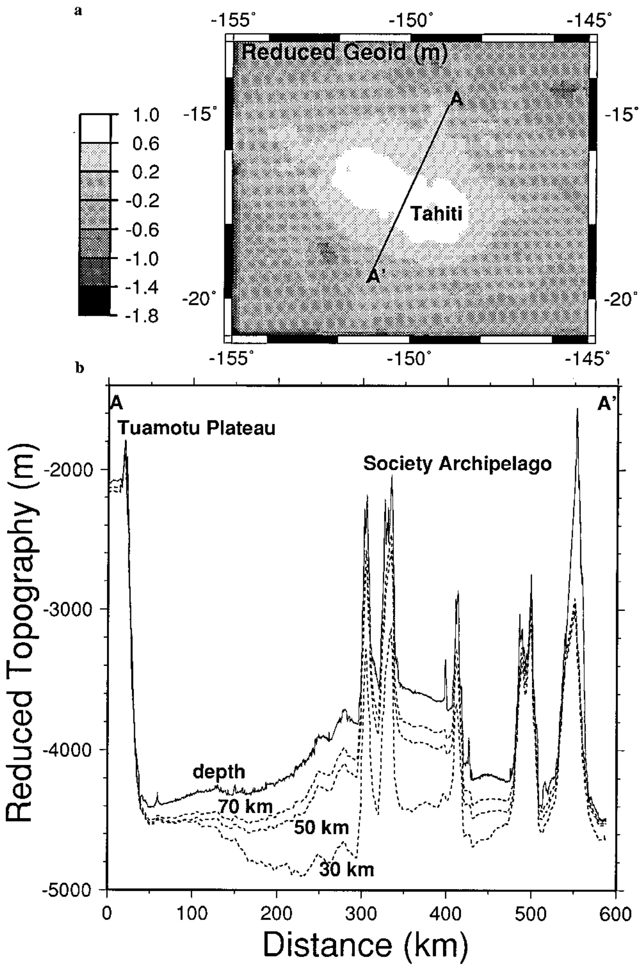

Figure 11. Geoid and depth of the Society Islands swell. (a) Contours of reduced geoid anomaly over the Society swell. The reduced geoid is the observed geoid minus the geoid predicted from the volcanoes and their isostatic compensation, assuming an elastic plate model. (b) Observed bathymetry (solid line) and reduced topography (dashed lines) along line A-A' across the Society swell. The reduced topography is the observed bathymetry minus the predicted swell topography, assuming that the geoid anomaly in Figure 11a is caused by uplifted seafloor compensated at 30, 50, and 70 km depths.

out for shallow compensation. Subtracting the predicted swell heights from the observed topography (Figure 11b) yields the reduced topography, what the bathymetry would look like if the swell were not there, as a function of the assumed compensation depth. The compensation depth can be adjusted until the reduced topography looks like volcanoes resting on otherwise flat seafloor. On the basis of this criterion a compensation depth of 30 km is too shallow, but 50 km is too deep. Although it is tempting to conclude from these shallow compensation depths that the lithosphere is thinner beneath the Superswell than beneath Hawaii, *Robinson et al.* [1987] have pointed out that in the presence of a low-viscosity zone, compensation depths of midplate swells can be underestimated. Since the long-wavelength geoid already establishes the presence of a low-viscosity zone in this region, swell compensation depths are inconclusive as to the thickness of superswell lithosphere.

3.5. Heat Flow

Heat flow is a measure of the heat being conducted up the geothermal gradient through the seafloor. The average heat flow over the South Pacific Superswell as a function of plate age is not resolvably different than other Pacific values (Figure 12), even though the depth of the seafloor at the heat flow sites on the Superswell is consistently shallower [*Stein and Abbott*, 1991]. At face value these observations support the interpretation that the lithosphere beneath the Superswell is not unusually

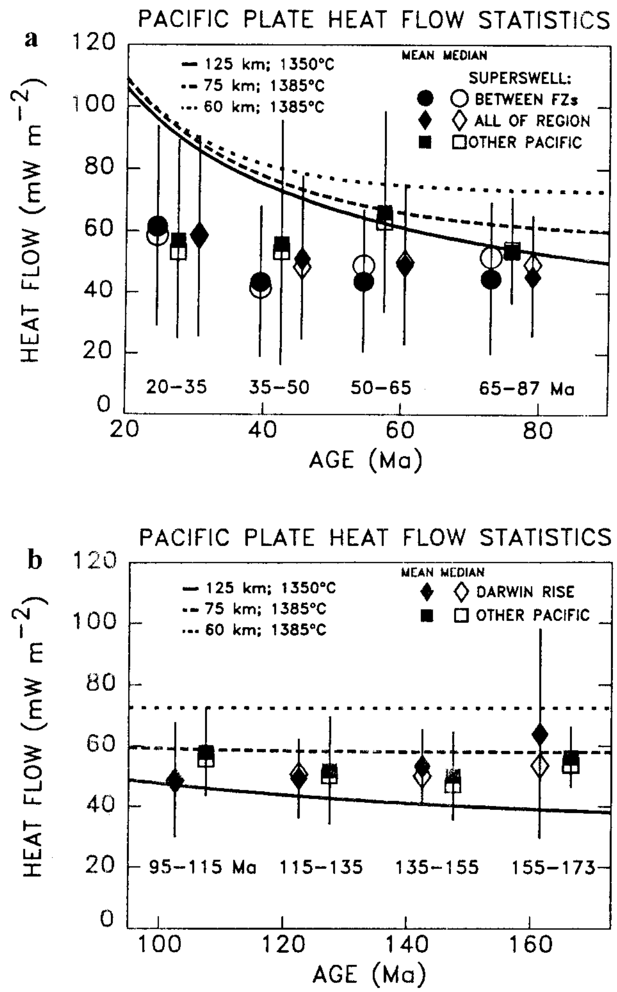

Figure 12. (a) Means (solid symbols), medians (open symbols), and standard deviations (vertical lines) of heat flow values in the South Pacific Superswell region (diamonds), a subset of the Superswell region that includes only the area between the Marquesas and Austral Fracture Zones (circles), and elsewhere on the Pacific plate (squares). (b) Same as Figure 12a but for the Darwin Rise in the North Pacific. Note the difficulty in resolving any difference in heat flow between superswell and nonsuperswell lithosphere or as a function of lithospheric age between 20 and 173 Ma (from *Stein and Abbott* [1991].

thin and hot. Nevertheless, elevated heat flow over the Superswell might be expected if the origin of the depth and geoid anomaly is elevated temperatures in the asthenosphere beneath the plate and if there has been sufficient time for the heat to be conducted to the surface. Thus the lack of a heat flow anomaly could imply either that the origin of the Superswell is nonthermal (e.g., convecting material beneath is low density by virtue of its mineralogy rather than its temperature) or that the hot material lies deeper than 60 km. The problem with the latter explanation is that the effect of the anomalous heat should eventually reach the surface within the ensuing 100 Myr. While this causes no concern for the Tertiary Superswell, it is a problem for the Cretaceous Darwin Rise, which has no heat flow anomaly either [*Stein and Abbott*, 1991], >100 Myr after volcanism began.

Before concluding that the only remaining explanation for superswells is a nonthermal source of buoyancy, we must address the bigger issue of why there is so little variation in heat flow with age, on or off the Superswell, and why the observed heat flow is systematically lower than the predictions of any conductive cooling relation (Figure 12). One possible explanation is that water circulation in ocean crust removes heat advectively out to ages beyond 50 Ma [*Stein and Stein*, 1994]. Heat flow measurements are typically made in sediment basins, which are predicted to be sites where cold seawater flows downward to recharge flow systems that vent warmer water near the base of basement outcrops. Since such flow systems are expected to be at least as vigorous on superswells as elsewhere on account of the large number of volcanic outcrops, the existing, sparse heat flow measurements are likely to be highly aliased with respect to resolving these circulation systems, making it difficult to conclude much about presence or absence of heat at depth.

A simple calculation shows that regardless of the buoyancy source for the depth anomaly, just the heat transported from the asthenosphere to the crust via magma advection to build islands and seamounts should be geologically significant. Let L be the latent heat of fusion for basalt (125°C when expressed as the temperature drop in the solid phase that would yield equivalent energy to the isothermal phase change), let ΔT be the temperature difference between the crust and the asthenosphere (1000°C), let C_p be the volumetric specific heat (4.125 MJ °C^{-1} m^{-3}), let h_t be the total volume per unit area of basaltic melt extracted from the mantle ($\approx 12h_{\mathrm{equiv}}$), and let t_v be the entire duration of volcanic activity on the Superswell (40 Myr). The average increment to heat flow q_b during this interval caused by the freezing and cooling of the magma is

$$q_b = C_p(L + \Delta T)h_t/t_v = 7.5 \text{ mW m}^{-2} \qquad (6)$$

This contribution to the heat flow should be apparent within 4 Myr of volcanism, given that the emplacement depth is shallow, and represents an increase of 15% in the background heat flux. Nevertheless, even this component of the heat transfer from the asthenosphere to the oceans has yet to be resolved in the heat flow data (Figure 12). Venting of heat on superswells is apparently not properly quantified by standard heat flow measurements, which only provide a lower bound to the actual heat flux.

3.6. Effective Elastic Plate Thickness

One of the more controversial proposals concerns the effective elastic thickness of superswell lithosphere. Figure 13 shows that in general, volcanoes that form on lithosphere between 50 and 90 Myr old show elastic plate thicknesses between 20 and 40 km [*Watts et al.*, 1980], except for the South Pacific Superswell where early studies concluded that the elastic plate thickness is <15 km [*McNutt and Menard*, 1978; *Cazenave et al.*, 1980; *Calmant and Cazenave*, 1986, 1987]. Modeling of gravity and bathymetry data collected by surface ships suggests that the elastic thickness of the Darwin Rise lithosphere (Figure 13) was unusually low at the time of volcanism as well [*Smith et al.*, 1989, *Wolfe and McNutt*, 1991]. Because the strain rate of rocks flowing in the ductile regime depends exponentially on temperature, the base of the elastic plate is thought to conform roughly to an isotherm between 450° and 600°C [*Watts et al.*, 1980]. Thus any thinning of the elastic plate over the Superswell should be accompanied by elevated temperatures in the upper portion of the lithosphere, which is in direct conflict with the normal heat flow values.

The solution to this paradox is that for several different reasons, early estimates of the elastic thickness of the lithosphere beneath superswell volcanoes appear to be too small. In a few cases, errors in the bathymetric data used to estimate elastic thickness from matching theoretical gravity or geoid anomalies to those measured with radar altimetry biased the results low [*Smith*, 1993]. For example, *Filmer et al.* [1993] calculated rather normal elastic plate thickness values of 18 ± 2 and 23 ± 2 km for the Marquesas and Society Islands, respectively, in French Polynesia using shipboard multibeam bathymetry and gravity data (Figure 13). The same analysis using readily available gridded digital bathmetry, such as ETOPO 5, yielded smaller elastic thicknesses because the mass of the island chains is systematically overestimated compared with that actually observed along ship tracks. However, errors in the bathymetric data are not the only explanation. The low estimates of elastic thickness from *Smith et al.* [1989] and *Wolfe and McNutt* [1991] for the Darwin Rise and from *Goodwillie* [1995] for the Pukapuka volcanic ridges on the Superswell were obtained using data of similar distribution and quality to those used by *Filmer et al.* [1993] to argue that the Superswell lithosphere is not everywhere anomalous in its elastic strength. With careful analysis of high-quality data the problem seems to be that both normal and

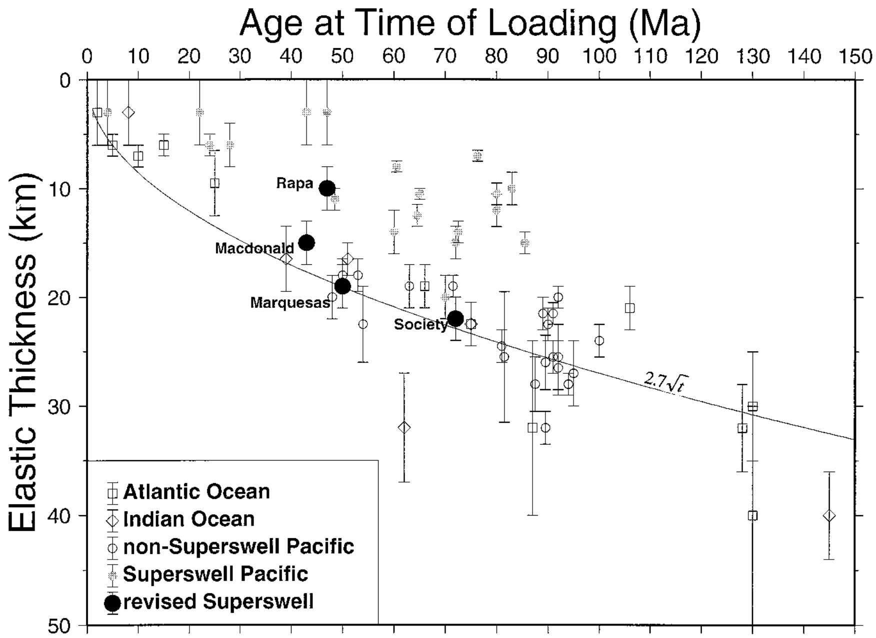

Figure 13. Effective elastic thickness of oceanic lithosphere as a function of the age of the plate at the time of loading as estimated for 60 examples in the three main ocean basins: Atlantic (open squares), Indian (open diamonds), non-Superswell Pacific (open circles), and Superswell Pacific (small stippled circles) as compiled by *Calmant and Cazenave* [1987] from many sources. Large solid circles show revised estimates for Tahiti, the Marquesas, Rapa, and Macdonald Seamount (all on the South Pacific Superswell) based on high-resolution shipboard bathymetry and gravity data. Tahiti and Marquesas data are from *Filmer et al.* [1993], while the Rapa and Macdonald estimates are from *McNutt et al.* [1997].

anomalously low values of elastic thickness are found on superswell lithosphere [*Goodwillie and Watts*, 1993].

The fact that volcanic centers in French Polynesia frequently remain intermittently active for long periods of time provides an attractive explanation for the conflicting opinions as to whether elastic plate thickness is or is not normal over superswells. Unlike the simple age-progressive model for Hawaii, in French Polynesia volcanic chains are frequently overprinted much later by renewed volcanism [*Duncan and MacDougall*, 1976; *Bonatti and Harrison*, 1976]. Even the lineated volcanic ridges on the Superswell appear to be most active at their eastern end near the EPR but then remain volcanically active well off ridge [*Shen et al*., 1993; *Sandwell et al*., 1995]. Samples from rock dredges used to date the features are biased toward the youngest volcanic event, but the elastic plate thickness is some weighted average of the thermal structure of the lithosphere when each load increment was emplaced. This effect has now been quite dramatically documented in the southern Austral Islands through dredging, dating, and elastic modeling of two nearly superimposed volcanic chains [*McNutt et al*., 1997]. The younger Macdonald chain loads an elastic plate with a normal elastic thickness, 15 km, for its age, 40 Ma. However, the fact that the chain sits on the flanks of a much larger, buried chain of ~30 Ma volcanoes produces an apparently low value for elastic thickness using lower-resolution data (Figure 14). This explains why the two volcanic chains in French Polynesia that appear to have "normal" values of elastic thickness are the Marquesas and Society Islands [*Filmer et al*., 1993], two Polynesian chains for which discordant ages, volcanic overprinting, and line-source volcanism have not been reported.

3.7. Isotopic Anomalies

An intriguing feature of the South Pacific Superswell is its correspondence with the South Pacific Isotopic and Thermal Anomaly (SOPITA) [*Staudigel et al*., 1991; *Smith et al*., 1989], a region of radiogenically enriched isotopes in the volcanic products. Because different isotopes of the same element behave in chemically identical ways throughout the process of melt fractionation and segregation, geochemists can use ratios of pairs of radiogenic to stable isotopes as preserved in volcanic rock as tracers to estimate how well mixed the mantle source is and to determine whether various hotspots tap distinct mantle source regions. As is shown in Figure 15, the Sr, Nd, and Pb isotopic ratios in magmas from the Superswell [*Vidal et al*., 1984; *White*, 1985; *Palacz and Saunders*, 1986; *Dupuy et al*., 1987] occupy much of compositional space between four extreme "end-members" in isotopic composition that characterize the mantle sources of oceanic volcanism worldwide [*Zindler and Hart*, 1986]: depleted MORB mantle (DMM), or the widespread depleted mantle source for mid-ocean ridge basalts (MORB), and three enriched components. Superswell volcanoes are so extreme in their diversity that

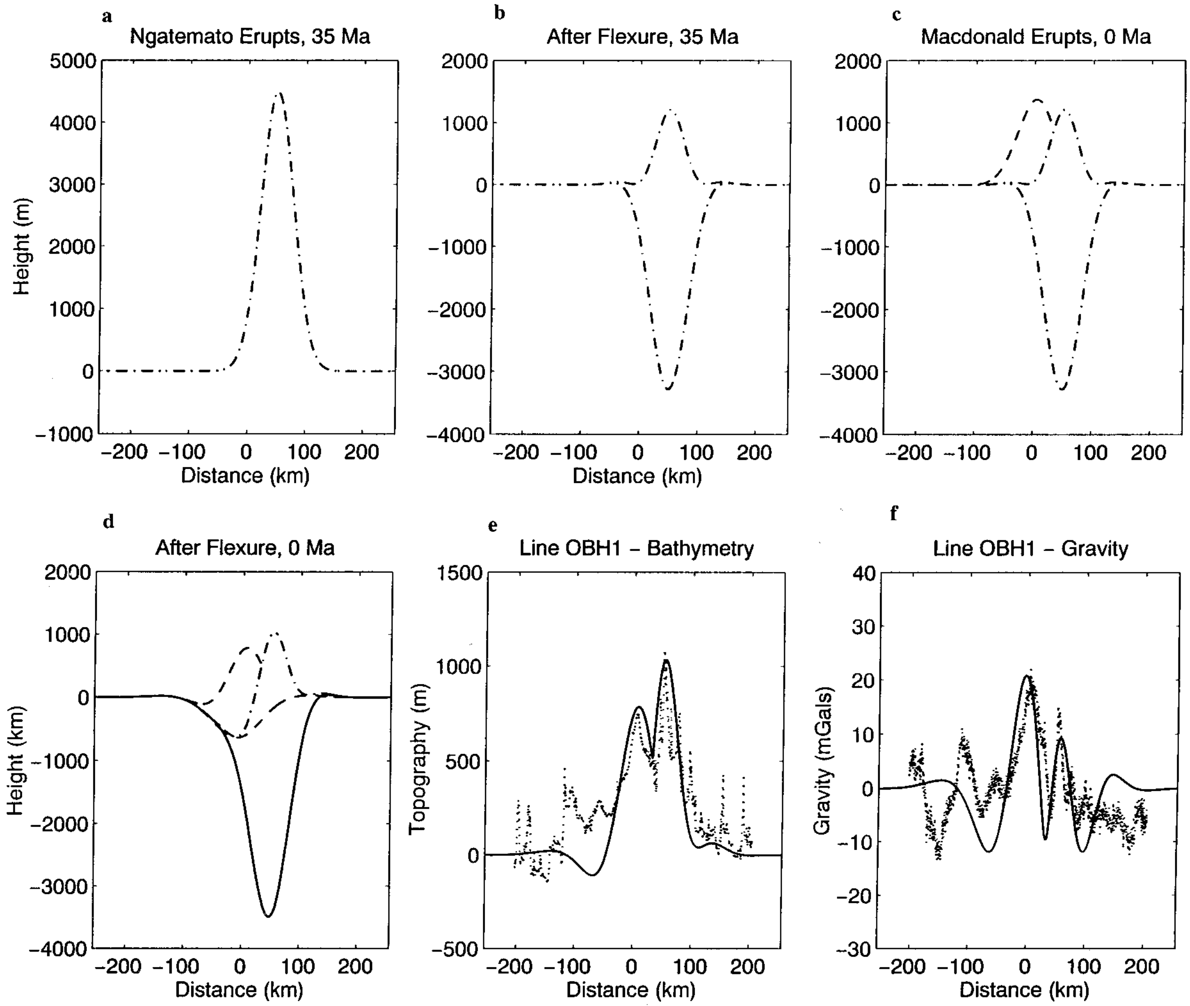

Figure 14. Elastic flexure model for two nearly superimposed seamount chains in the southern Australs near Macdonald seamount. (a) The older (~30 Ma) seamount erupts, creating a 4.5-km load. (b) After flexing the lithosphere the net height of the seamount is small on account of the deep moat it produces on a weak elastic plate. (c) A young (~0 Ma), small (1.5 km high) seamount (dashed line) erupts on the flanks of the old chain, (d) The young chain flexes a stiffer elastic plate (dashed line). The solid line shows the combined effects of flexure from the two loads. (e) The final topographic profile from the two loads (solid line) provides a reasonable match to the bathymetry along a line perpendicular to the southern Austral seamount chain (dots). The small difference in the net height of the two chains despite their very different eruptive volumes is explained by the difference in stiffness of the elastic plate for the young and old loads. (f) Net predicted gravity anomaly (solid line) obtained from the density effects of the topography in Figure 14e (solid line) and the depression of the crust-mantle boundary predicted from the plate bending in Figure 14d (solid line) is compared with the observed gravity anomaly (dots). Note that the smaller volcano on the left produces a larger gravity anomaly since it is supported by a stiffer plate. From *McNutt et al.* [1997]; copyright 1997 Macmillan Magazines Ltd.

they actually define two of the enriched end-member components: (enriched mantle II) (EMII) and high $\mu = {}^{238}U/{}^{204}Pb$ (HIMU). The EMII end-member is characterized by low $^{143}Nd/^{144}Nd$, high $^{87}Sr/^{86}Sr$, and high $^{207}Pb/^{204}Pb$ and $^{208}Pb/^{204}Pb$ at a given value of $^{206}Pb/^{204}Pb$. The HIMU end-member is characterized by high $^{206}Pb/^{204}Pb$, $^{207}Pb/^{204}Pb$, and $^{208}Pb/^{204}Pb$ at relatively low $^{87}Sr/^{86}Sr$ [*Zindler and Hart*, 1986]. At least in the Marquesas chain the HIMU source dominates in the earlier lavas, which result from larger degrees of partial melt at shallower depths, while the EMII source is more apparent in the later stage lavas that melted at deeper levels [*Desonie et al.*, 1993].

The radiogenic enrichment of the EMII end-member requires that its source have high concentrations of the radioactive parents, U and Rb. Given that both of these elements are highly enriched in continental crust, one possible pathway for this enrichment is to transport continental crust or continent-derived sediment into the mantle via subduction [*Anderson*, 1982]. The HIMU end-member may also have a subduction connection: Its isotopic ratios could be produced by subduction of an-

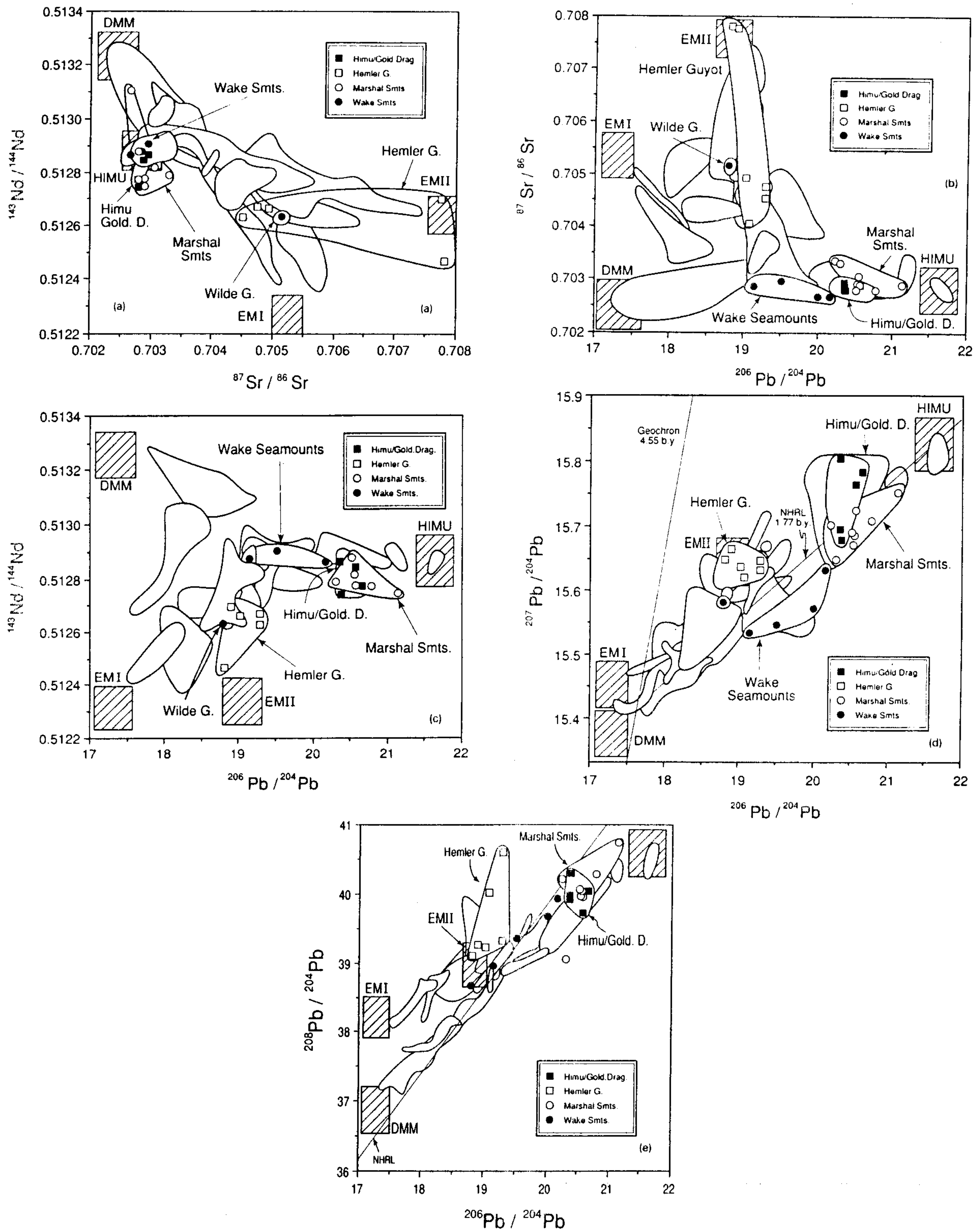

Figure 15. Isotope correlation diagrams of Nd, Sr, and Pb for rocks from the Darwin Rise (symbols) superimposed on isotopic fields (free-form closed loops) defined by rock samples from the Darwin Rise. Reprinted from *Staudigel et al.* [1991] with kind permission of Elsevier Science–NL.

cient oceanic crust that was altered by extraction of island arc tholeiites [*Zindler and Hart*, 1986]. Whatever the source of these anomalies, they provide a geochemical "fingerprint" for a mantle source region that is also seen in Cretaceous rocks dredged from the Darwin Rise, in terms of both the diversity and the extreme compositions (Figure 15).

Several generalizations can be drawn from the isotopic anomalies. The enrichment must have occurred >100 Myr ago, on the basis of the age of the Darwin Rise, and this radiogenic enrichment might provide some portion of the heat source for the Superswell. The diversity in compositions points to a heterogenous, poorly mixed source for the melts. One suggestion for explaining the evolution in isotopic anomalies from HIMU to EMII in the Marquesas is to suppose that a mantle plume with EMII composition melts a HIMU upper mantle [*Desonie et al.*, 1993]. Another possibility is that the upper mantle beneath superswells is enriched in Pb isotopes but otherwise radiogenically diverse on smaller scales. That diversity shows up in the volcanic products because only small degrees of partial melt of small volumes of the mantle are involved in producing each volcano.

3.8. Plate Reconstructions

Henderson [1985] calculated poles of rotation that track the drift of the Pacific plate with respect to the hotspots over the past 135 Myr. Whereas *Menard* [1984] had only suggested that the Darwin Rise at 100 Ma was like French Polynesia today, Henderson's reconstructions put the Darwin Rise over the French Polynesian hotspots at 100 Ma. Magnetic paleolatitudes calculated for the Cretaceous Darwin Rise volcanoes (Figure 16) also place the region in the South Pacific at the time of volcanism [*Winterer et al.*, 1993], although there is some suggestion of a few degrees drift south of the hotspots with respect to the geomagnetic dipole axis.

One reasonable explanation for why this particular area of Earth is so prone to excess volcanic activity is that since the Mesozoic, this region of the mantle has been free of subduction [*Anderson*, 1982]. The plates of the Pacific Ocean have all been underthrusting beneath the bordering continents in a direction away from the central Pacific. This connection becomes even stronger when one recognizes that Africa, the site of another proposed superswell, has also lacked underthrusting plates for 100 Myr or more. Subduction inevitably acts to cool the surrounding mantle, and thus absence of it would lead to anomalously warm mantle when compared with the planetary average. This theory, however, conflicts with the notion that the radiogenic enrichment of the isotopes on superswells is produced by subduction, unless the enrichment is very much older than 100 Ma or was produced elsewhere and transported by mantle convection to the site of superswell volcanism.

3.9. Seismic Velocities

Slow seismic velocities for shear waves [*Su*, 1992] underlie the South Pacific Superswell from the surface down to 450 km (Figure 17). The dependence of Love-wave phase-velocity anomalies on period also suggests that slow shear wave velocity is concentrated in the uppermost mantle beneath the Superswell [*Nishimura and Forsyth*, 1985; *McNutt and Judge*, 1990]. In the upper 150 km the slow velocities are highly correlated with the

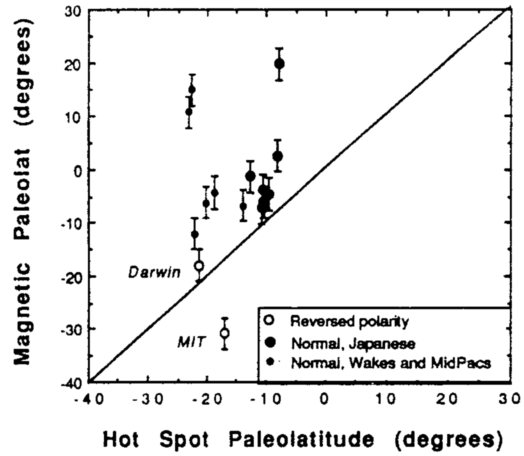

Figure 16. Magnetic paleolatitude for Darwin Rise guyots plotted versus predicted paleolatitude based on estimates of the motion of the Pacific plate with respect to hotspots and age of the volcano from dredge samples. From *Winterer et al.* [1993].

pattern of shallow depth (Figure 3). The pattern of geoid anomalies, with the low striking strongly in the direction of absolute plate motion, is most correlated with the pattern of seismic velocities at 450 km, with slow velocities corresponding to geoid lows.

On the basis of data from the recent Mantle Electromagnetic and Tomography (MELT) Experiment the EPR marks a major discontinuity in anomalous seismic structure, similar to the discontinuity in subsidence rate noted in section 3.2. The propagation of surface (Rayleigh) waves to ocean bottom seismometers located on and near the EPR is very slow for events crossing the Superswell as compared with events crossing Nazca lithosphere of the same age. Shear velocities are low enough that melt may be present on the Superswell side of the ridge out to at least 5 Ma [*Forsyth et al.*, 1996]. These data suggest that the anomalous behavior of the Superswell is produced by the absolute motion of the plate over the mantle, since this is the property that changes suddenly and drastically at the EPR [*McNutt and Judge*, 1990], with the Pacific plate drifting rapidly to the west-northwest and the Nazca plate drifting more slowly to the east.

The size of the velocity anomalies beneath the Superswell is generally from −1.2 to −0.5%. If the anomalies arise solely from temperature variations in the upper mantle, the implied thermal anomalies underlying the Superswell are of the order of +20° to +40°C averaged over distances of several thousand kilometers. However, there is no guarantee that the cause of the slow seismic velocities is temperature changes. Variations in mantle mineralogy, enhanced volatile content, and the presence of small degrees of partial melt can all lead to shear wave velocity anomalies.

Unfortunately, we have no way of determining the seismic velocity structure of the mantle beneath the

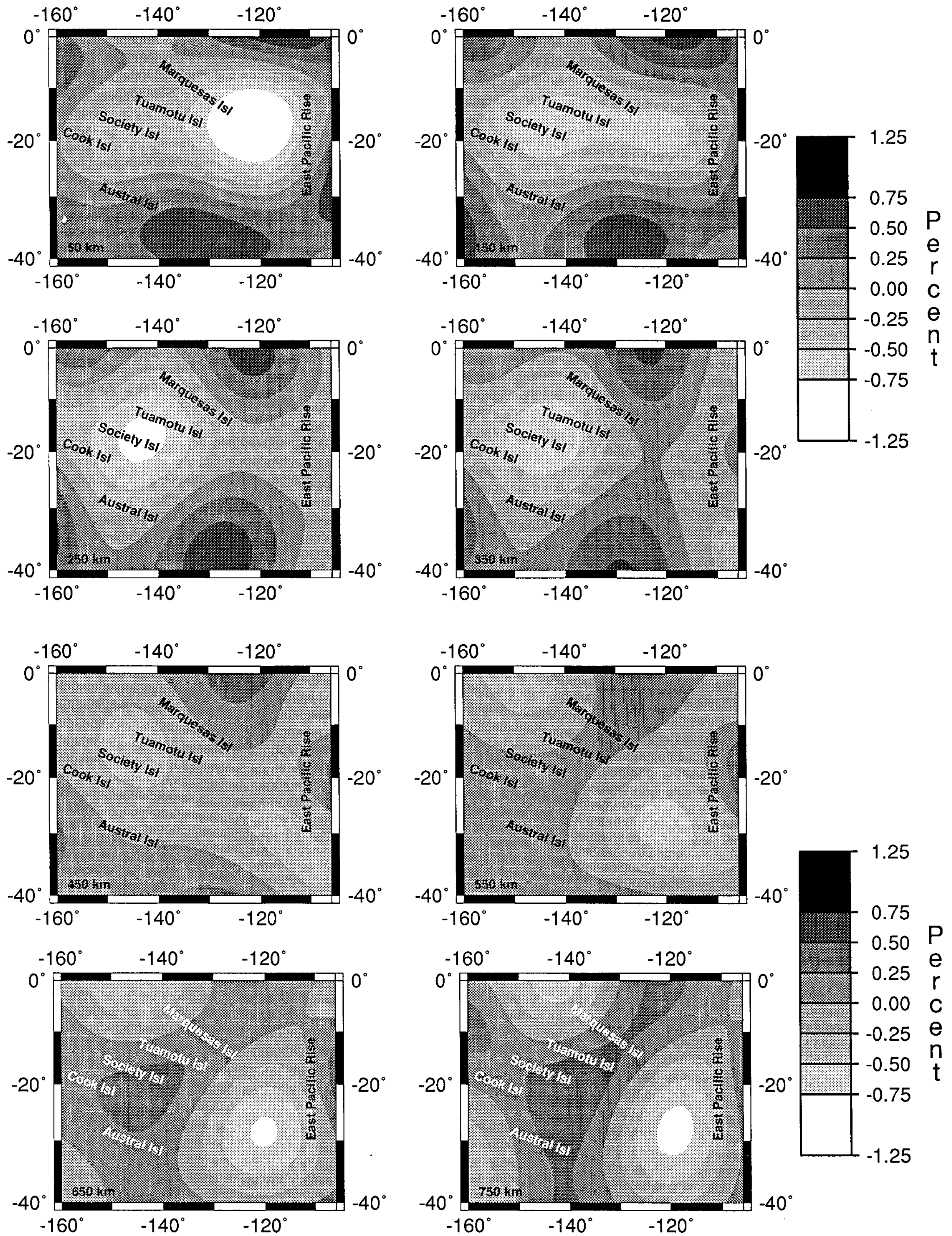

Figure 17. Shear wave velocity anomalies [*Su*, 1992] beneath the South Pacific Superswell at depths of 50–750 km. The model includes coefficient for spherical harmonic degrees 2–12 (wavelengths 20,000–3000 km), but the long-wavelength components (20,000–6000 km) have been removed as they vary only on space scales larger than that of the Superswell. The model is represented in the radial direction by a degree 13 Chebyshev polynomial, which corresponds to an average resolution of 200 km in depth.

Darwin Rise when it was active at 100 Ma. Figure 18 shows the *S* wave velocity structure beneath the North Pacific today [*Su*, 1992] (although the higher resolution model of J. Ekstrom (personal communication, 1995) is very similar). As is the case for the Superswell, slow seismic velocity is associated with the Tertiary volcanism, in this case the Hawaiian chain, to the point of even deviating northward at 170°E to follow the early Tertiary trace of the Emperor Seamounts. However, the dimension of the Hawaiian anomaly is small compared with that of the Superswell. The older Cretaceous volcanic chains such as the Japanese, Marcus-Wake, Mid-Pacific, Marshall, and Magellan Seamounts are underlain by slightly fast material. As is the case for the South Pacific, the bathymetry variations are similar in pattern to the seismic velocities in the uppermost mantle, although the signal is not so large or striking as it is in the South Pacific. There is again an excellent correlation between the pattern of geoid anomalies and velocity, with geoid highs corresponding to velocity highs, but the depth at which the correlation occurs is much deeper, 650–750 km.

4. THE AFRICAN SUPERSWELL

Africa has long been known to be anomalously elevated on the basis of average continental hypsography (distribution of area with depth) [*Harrison et al*., 1983], with southern and eastern Africa being the primary contributors to the anomalous elevation. *Nyblade and Robinson* [1994] noted anomalously shallow depths in the adjacent southern Atlantic Ocean and proposed that these areas together (Figure 1) form another modern-day superswell with amplitude of 500 m. Like the central Pacific, the mantle beneath Africa has not experienced Cenozoic subduction, but in almost all other respects the African plate is very different from the Pacific plate (mostly ancient continental crust, slowly moving in any absolute reference frame, etc.). Thus the establishment of Africa as a superswell would argue strongly against the suggestion based on the Nazca-Pacific discontinuity in seismic velocity and subsidence rate at the EPR that rapid motion of a plate with respect to the mantle is a primary factor in the formation of a superswell.

If the African superswell is similar in origin to its Pacific namesake, we would expect the region to be characterized by a concentration of intraplate volcanism, slow seismic velocities in the upper mantle, and possibly a dip in the geoid. On the basis of *Burke and Wilson*'s [1972] compilation of hotspots, there are 17 sites of active or recently active volcanism on the African plate, of which 11 fall within the boundaries of the African superswell. Two of these hotspots lie along the east African rift system, and most of the others are near the southern Mid-Atlantic Ridge. In terms of plume flux [*Sleep*, 1990] these 11 hotspots are very minor, together accounting for only one of the South Pacific Superswell's hotspots in intensity. Nevertheless, the African plate does display a large number of hotspots by any continental standard.

The seismic velocity structure is less supportive of an upper mantle origin for the high elevation of Africa. Global seismic studies [*Su*, 1992; *Zhou*, 1996; J. Ekstrom, personal communication, 1995] show that slow velocities in the African upper mantle are limited to the region of the East African Rift (Figure 19). Southern Africa and the adjacent region of the Atlantic are anomalously fast well down into the transition zone. On the basis of heat flow observations, *Nyblade and Robinson* [1994] originally had attributed a large part of the uplift of the African superswell to heat at lithospheric depths. However, a later analysis of seismic velocities in the uppermost mantle beneath southern as compared with central Africa [*Nyblade et al*., 1996] ruled out any substantial amount of lithospheric thinning.

The geoid as well does not support a strong similarity between Africa and the South Pacific. A region of low geoid height is limited to a band striking east-west through the East African Plateau. Southern Africa and the adjacent Atlantic display a geoid high. Therefore although this region of Africa qualifies as a superswell by virtue of its high elevation and enhanced rate of mid-plate volcanism, it lacks many of the other distinctive features of the South Pacific Superswell that are diagnostic of its origin.

5. MODELS FOR SUPERSWELL FORMATION

Using the constraints listed in section 3, one can consider several possible mechanisms for forming a topographically elevated superswell: (1) pure lithospheric thinning via stretching the plate [*Sandwell et al*., 1995]; (2) chemical buoyancy through spreading of a layer of mantle depleted by plumes [*Phipps Morgan et al*., 1995]; and (3) dynamic support through upwelling in convecting mantle [*McNutt and Judge*, 1990; *Larson*, 1991a, b, *Davies and Pribac*, 1993].

As long as the stretched crust in explanation 1 is rethickened by off-ridge volcanic activity, this mechanism produces a superswell by increasing the thermal gradient in the stretched lithosphere. Consequences of the stretched lithosphere would be heat flow anomalies and reductions in the elastic plate thickness. As was discussed in section 3, these features are probably not present on the South Pacific Superswell. In addition, this explanation can be ruled out as the sole cause of a superswell because it would not produce a geoid low over French Polynesia or excess volcanism over what is required to rethicken the thinned crust to the 6-km value produced at mid-ocean ridges (without some other heat source or way to reduce the melting temperature). While some modest amounts of extension may help the formation of long, non-age-progressive island chains by producing cracks in the plate, an upper bound on the

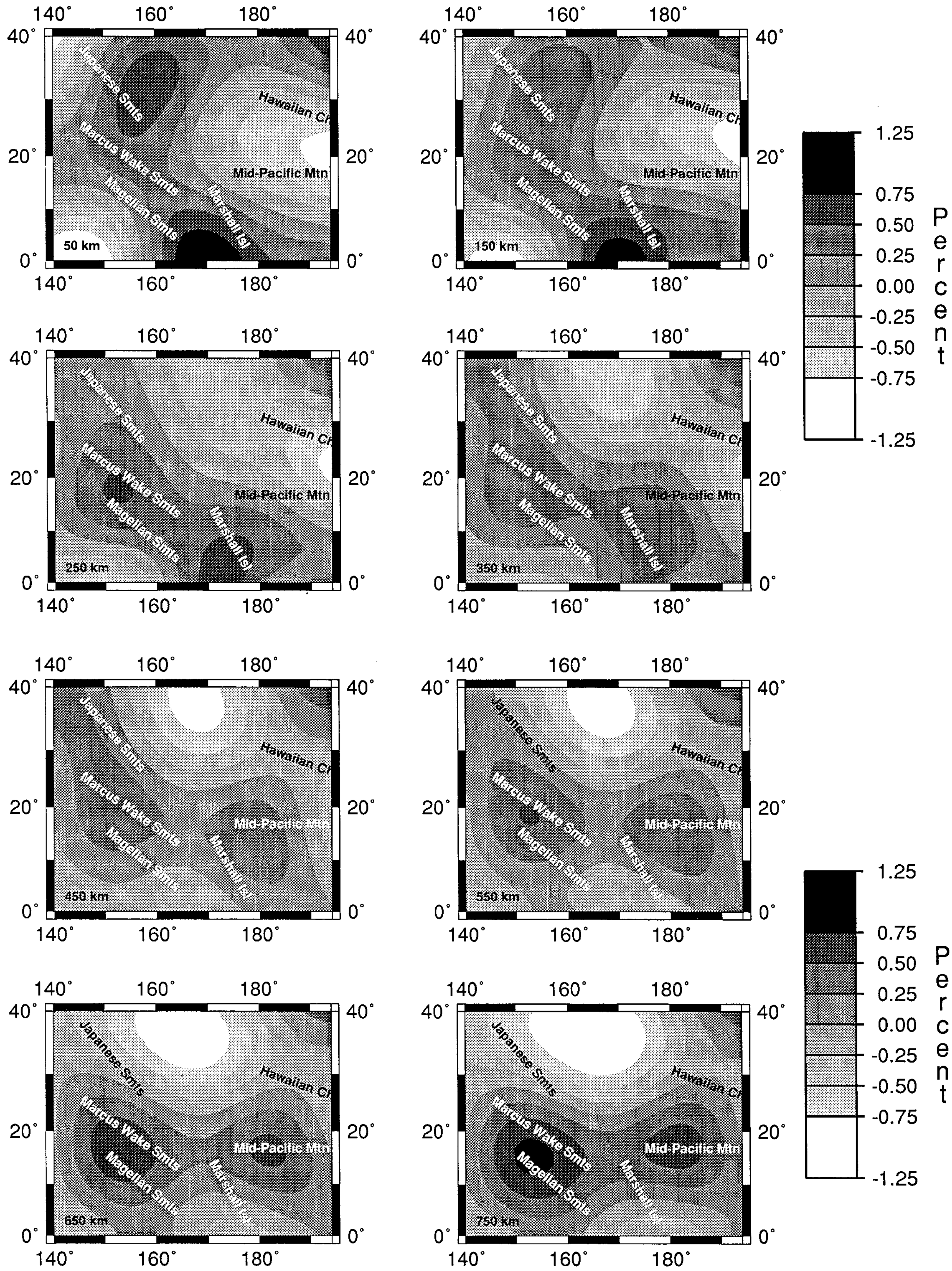

Figure 18. Shear wave velocity anomalies [*Su*, 1992] beneath the Darwin Rise at depths of 50–750 km and wavelengths 3000–6000 km (spherical harmonic degrees 7–12).

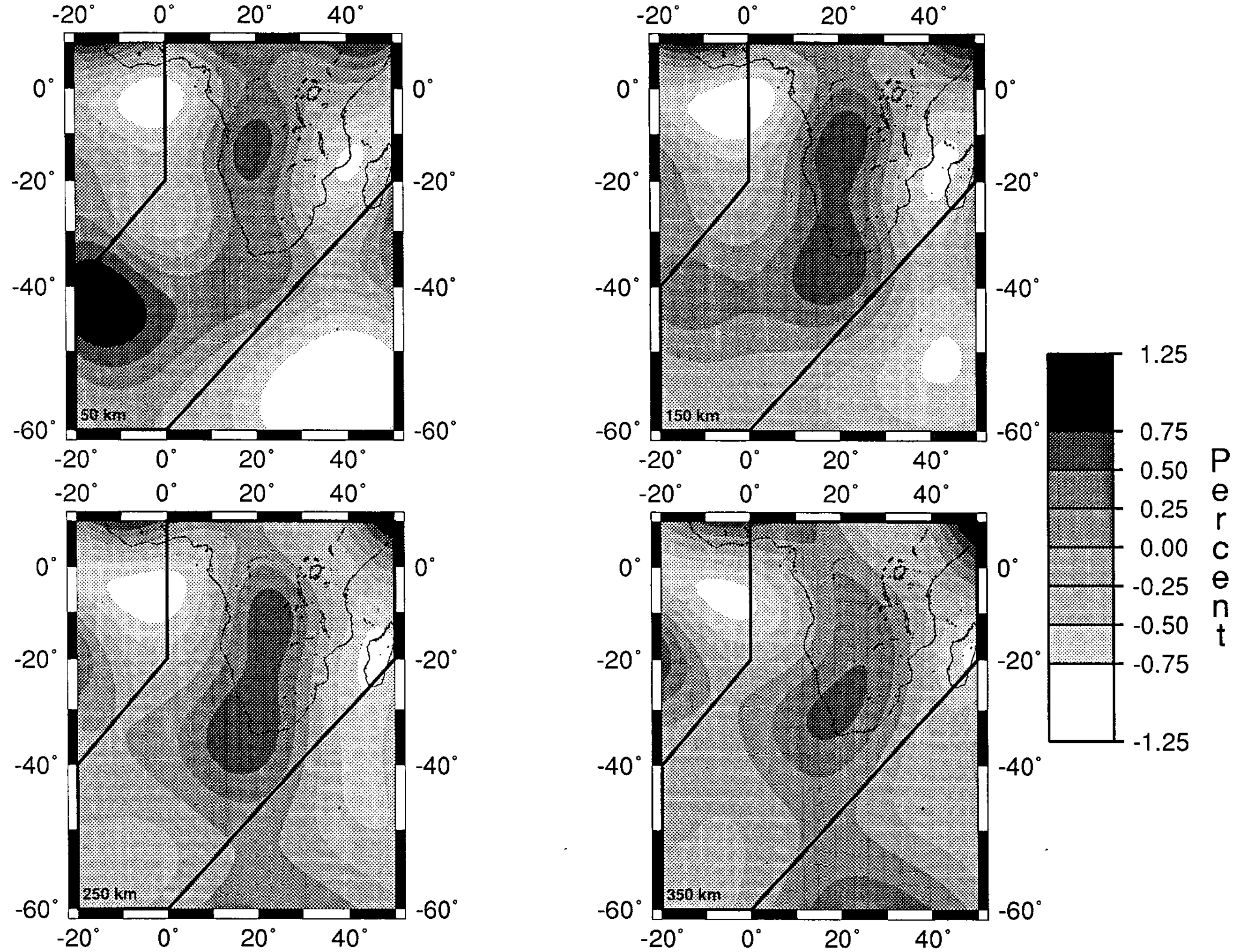

Figure 19. Shear wave velocity anomalies [*Su*, 1992] beneath southern Africa at depths of 50–350 km and wavelengths 3000–6000 km. Black lines outline the African superswell.

amount of stretching based on the lack of significant deformation of the Pacific fracture zones is only 65 km [*Goodwillie and Parsons*, 1992].

According to explanation 2, a regional depth anomaly could be produced by spreading of buoyant, depleted mantle created by plume volcanism. This model can also be quickly dismissed as the only cause. First of all, it does not explain why volcanism on superswells is enhanced at all scales. One would suspect that other sorts of midplate volcanism would be less likely to occur on account of displacement of fertile mantle by depleted mantle. Second, depleting the mantle increases its seismic velocity, in contradiction to the seismic images beneath the Superswell. Third, this mechanism does not produce a geoid low.

By default, explanation 3 has been the preferred explanation for both the uplifted seafloor and the excess volcanism. In particular, the geoid low correlated with uplifted seafloor on the Superswell is difficult to produce by any nonconvective mechanism. Now that seismic tomography has sufficient resolution to image the mass anomalies driving convection at the scale of a superswell, it is possible to test this model directly using depth and geoid constraints.

5.1. Dynamic Modeling

Assume that the seismic velocity anomalies shown in Figures 17 and 18 are density anomalies driving convection in a viscous mantle. Then, theoretical predictions of dynamic topography and geoid can be computed from the velocity anomalies using the principles of continuum mechanics [*Hager and Clayton*, 1989], given some assumptions of $d\rho/dv$, the conversion factor from seismic velocity anomaly to density anomaly, and the viscosity structure of the mantle. The theoretical dynamic topography is simply the uplift caused by the vertical normal forces at the surface caused by convection driven by the seismically imaged density anomalies. The geoid anomaly is the sum of the effects on the geopotential from the density anomalies themselves, the dynamic topography they induce, and the warping of any subsurface density interfaces caused by the convection.

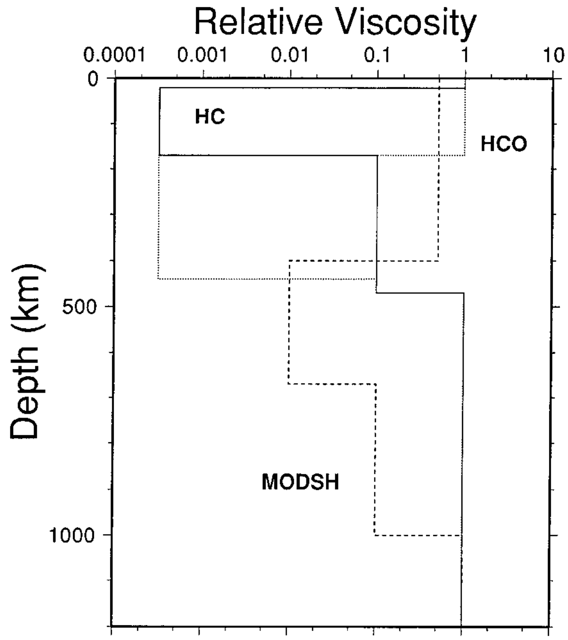

Figure 20. Three viscosity models used to predict dynamic topography and geoid for superswells. The HC model (solid line) is from *Hager and Clayton* [1989]. The HCO model is extremely similar to HC, except that a 120-km-thick lithospheric lid is placed on top of the model, forcing the low-viscosity zone deeper into the upper mantle. The MODSH model is from *King and Masters* [1992]. All models have unit viscosity from 1000-km depth to the core-mantle boundary.

The predicted dynamic topography and geoid will vary dramatically depending on the viscosity model chosen for the mantle. The way in which they vary is summarized by topography and geoid "kernels," which can be thought of as depth- and wavelength-dependent weighting functions that describe how the density anomaly at a given depth influences the surface depth and geoid anomaly at that particular wavelength. In general, all topography kernels peak in the shallow upper mantle so that a low-velocity riser near the Earth's surface causes surface uplift. All geopotential kernels are exactly zero at the surface (because the effect on the geopotential from a mass anomaly at that depth is exactly offset by that from the surface deformation it induces) and peak at deeper levels. Therefore it is no surprise that the depth variations on the South Pacific Superswell and Darwin Rise look like the seismic velocity anomalies in the uppermost mantle, while the geoid is correlated with deeper seismic structure. For the purpose of calculating topography and geoid, only ratios of viscosity variations with depth figure into the analysis. The absolute values matter only if one wishes to calculate mantle flow velocities, uplift rates, etc.

Given the infinite number of possibilities for mantle viscosity models, only models that had been validated by producing a reasonable fit to the long-wavelength (>10,000 km) geoid were considered here. While such models are by no means exhaustive, at least this procedure avoids the pitfall of producing a model that fits observations at wavelengths of 3000–6000 km characteristic of superswells but not at longer wavelengths. Most of these models fall into one of two categories: models with a low-viscosity zone immediately below the lithosphere (HC in Figure 20) and models with a low-viscosity zone in the transition zone (MODSH in Figure 20). Also shown in Figure 20 is a slight variant of the HC model, HCO, which also includes a low-viscosity zone below the lithosphere but allows for a much thicker plate.

Figure 21 shows the topography and geoid kernels for these models. They all show that at the wavelengths represented by superswells, the observations are primarily influenced by mass anomalies above 1000-km depth; the kernels all taper to zero below this depth. The topography kernels for the models with low-viscosity zones in the upper mantle fall off more quickly with depth than the MODSH model, but overall the topography kernels are similar. The geoid kernels show the greatest variation. On the basis of the location of the major peaks the HC model predicts a geoid that looks like the inverse of the seismic anomalies at 300–500 km. For the HCO model the geoid is also reversed in sign (negative geoid for a rising mass anomaly), but the greatest contribution comes from deeper in the mantle at 400- to 700-km depth. The MODSH model produces a positive geoid anomaly for a buoyant mass located anywhere above 700 km. On the basis of these simple observations and the correlations between seismic velocity and geoid mentioned earlier, we would expect the Superswell data to be fit by the HC model and the Darwin Rise to be fit by the HCO model.

These kernels can then be used to predict dynamic topography and geoid, given the seismic velocity anomalies and some value for $d\rho/dv$. In general, $d\rho/dv$ could vary with depth within the mantle, but since the variation cannot be constrained from independent data, here it is assumed constant. *McNutt and Judge* [1990] derived a value of -0.618 ± 0.108 m s^{-1} °C^{-1} for dv/dT, the change in shear wave velocity with temperature, based on a least squares fit to Love-wave phase velocities as a function of lithospheric age. Assuming that this is a representative value for the upper mantle and that $d\rho/dT = -\rho_s\alpha$, where α is the coefficient of thermal expansion (3×10^{-5} °C^{-1}), $d\rho/dv = 0.166$ kg s m^{-4}.

No corrections have been made for variations in lithospheric age in the data (Figure 3) by removing depth/age and geoid/age functions or in the models by not including seismic velocity anomalies near the surface. This procedure avoids the possibility of removing a convective signal through an inappropriate choice of reference model for the lithosphere or the possibility of trying to force a convective explanation for anomalies caused by temperature variations within the lithosphere. This does mean, however, that what is loosely called "dynamic topography" is the sum of the signals from expansion and contraction of the thermal boundary layer

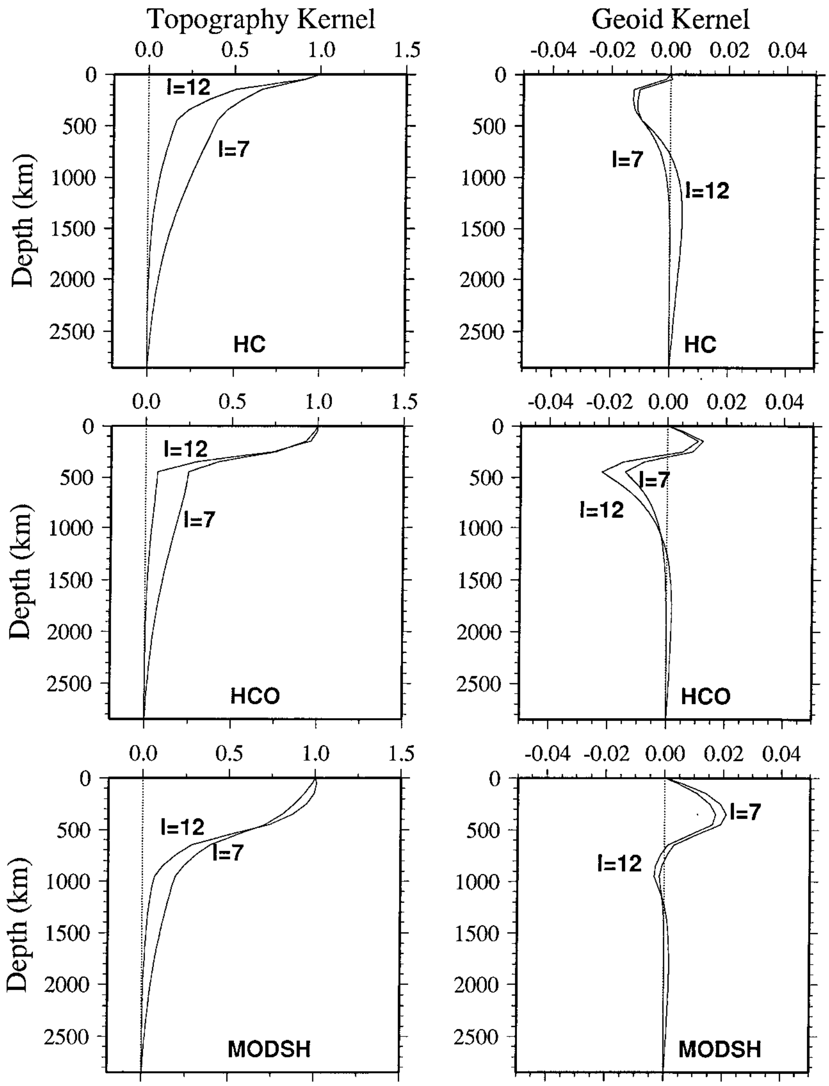

Figure 21. Topography and geoid kernels for models HC, HCO, and MODSH. The sign of the kernels has been plotted to show the effect of a buoyant mass anomaly on topography or geoid; for example, a rising, buoyant mass anomaly located at 400-km depth produces surface uplift and a negative geoid anomaly assuming the HC model and surface uplift but a positive geoid anomaly assuming the MODSH model. The $l = 7$ kernel corresponds to the depth-dependent weighting function for density anomalies of ~6000-km wavelength, while $l = 12$ corresponds to wavelengths of ~3000 km.

as well as vertical stress on the base of the lithosphere from flow in the mantle.

Figures 22–24 show the predicted dynamic topography and geoid over the Superswell and Darwin Rise assuming the three viscosity models in Figure 20. Of the three, model HC is the only one that produces a geoid low over the Superswell (Figure 22). The predicted variation in bathymetry and geoid match the observed variations well, demonstrating an appropriate choice of $d\rho/dv$. The pattern is also a reasonable match, given that this is at the edge of resolution of the seismic tomography, demonstrating that the HC viscosity model produces kernels that peak at the right depth with the correct sign. The predicted depth of old seafloor is shallower than that actually observed, a problem caused by the difficulty in resolving the actual depths of the thermal anomalies in the uppermost 100-km layer of the model, where the topography kernel is large. We arbitrarily assigned the slow velocities in the uppermost, 100-km-thick layer to 50-km depth; putting the anomaly near the base of the layer would reduce the shallow contribution by a factor of 2 and produce a better fit. The effect of this uppermost layer on the geoid is not important, since the geoid kernel is zero near the surface.

This same viscosity model HC is less successful in predicting the signal over the Darwin Rise. Discounting the island arcs and plateaus in Figure 3 leaves little variation in dynamic topography in this region to be predicted. However, the geoid signal is strong, and the east-west trending high through the Wake and Mid-Pacific seamounts is poorly matched by the HC prediction.

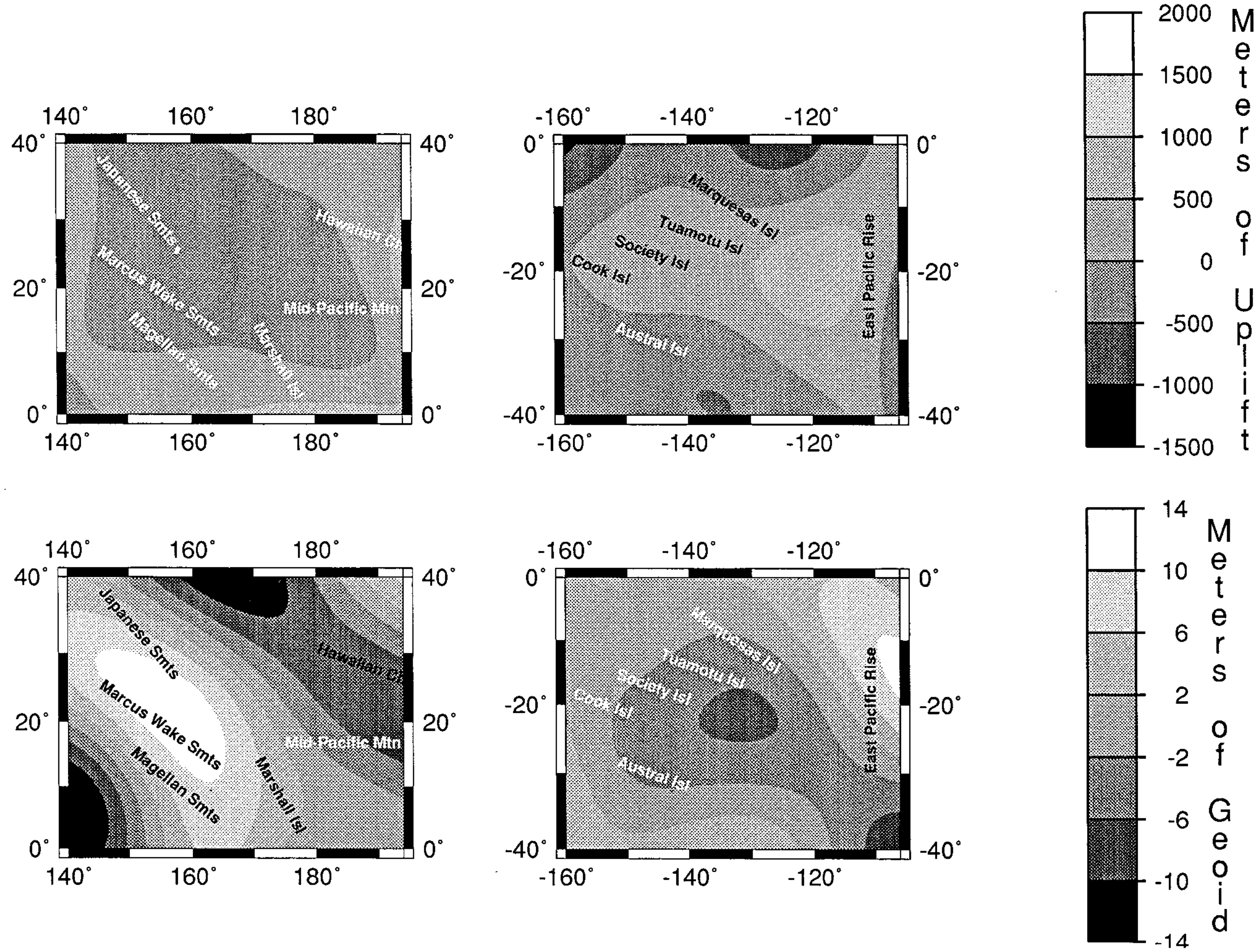

Figure 22. Predicted dynamic topography (all wavelengths down to 3000 km) and geoid (wavelengths 3000–6000 km) for the Darwin Rise and the South Pacific Superswell using the seismic velocity model of *Su* [1992] and the viscosity model HC [*Hager and Clayton*, 1989]. The mean from each grid was removed before display.

Adding a thicker lithospheric lid as in the HCO model produces geoid kernels which peak deeper in the mantle and thus provide a very reasonable fit to the geoid over the Darwin Rise (Figure 23). The predicted geoid matches the observed well except near Japan in the northwest corner of the grid. Since subducting slabs are poorly resolved in this tomographic model, this misfit is not surprising. This model with the thicker lithospheric lid, however, does not predict a geoid low over the hotspot chains on the Superswell. Thus even from the perspective of this geodynamic analysis, the lithosphere in the North Pacific, where the seafloor ranges in age from 100 to >160 Ma, is resolvably thicker than the lithosphere of the South Pacific, which ranges in age from 0 to 100 Ma. Thus lateral variations in viscosity within even a region as geologically homogeneous as the Pacific basin are required in order to fit depth and geoid data at 3000- to 6000-km wavelengths.

By comparison, the MODSH model (Figure 24) fits neither the sign nor the pattern of geoid anomalies over the Darwin Rise or the Superswell, even though it produces a reasonable fit to the global geoid at longer wavelengths [*King and Masters*, 1992]. This model with such a deep low-viscosity zone is more appropriate for continental than oceanic regions, and in fact, a slight variant on it produces an excellent fit to the geoid over the African superswell (M. G. Kogan and M. K. McNutt, Viscosity of the upper mantle: Continent versus ocean differences, submitted to *Journal of Geophysical Research*, 1997).

On the basis of the modeling results presented above, superswells can be explained as dynamic features caused by hot, buoyant material in the upper few hundred kilometers beneath the plate. Figure 25 shows the partitioning between "lithospheric" ($z \leq 85$ km) versus "asthenospheric" ($z > 85$ km) sources for the anomalies. The lithospheric signal in the depth consists of monotonic deepening of the seafloor from the EPR westward. The predicted slopes of the seafloor are symmetric about the position of the EPR. This is presumably the conductive cooling signal. In comparison, the asthenospheric part of the depth signal is asymmetric about

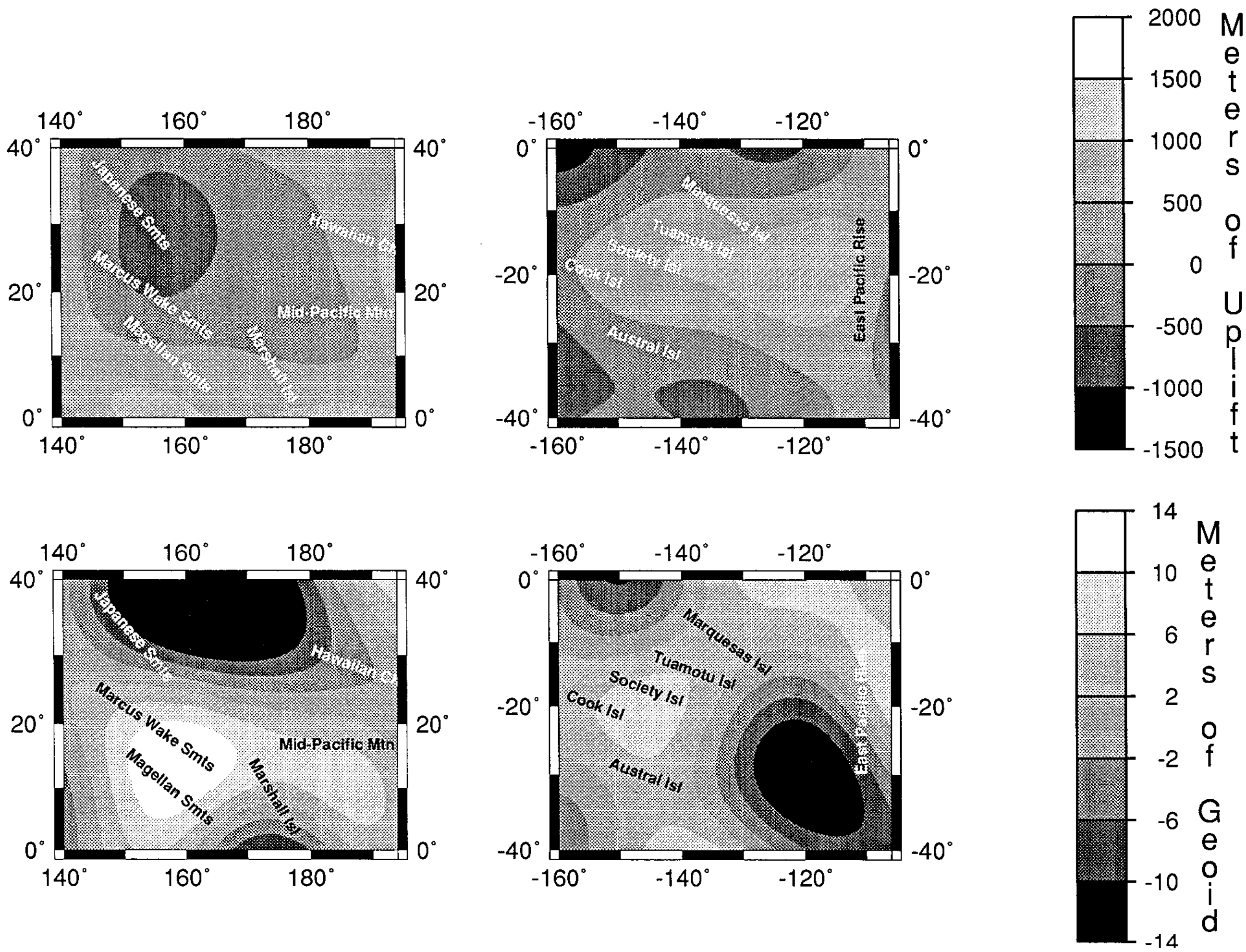

Figure 23. Predicted dynamic topography and geoid as in Figure 22, but assuming viscosity model HCO.

the EPR and produces the actual shoaling of the seafloor well off ridge with respect to the EPR, in agreement with the observations (Sichoix et al., submitted manuscript, 1997). The entire geoid signal is from sublithospheric depths (Figure 25), a consequence of the fact that at these wavelengths, mass anomalies in the lithosphere are isostatically compensated.

The difference between active and fossil superswells can be explained by thickening of the lithospheric lid and commensurate deepening of the low-viscosity zone, perhaps through drift of the plate off the anomalously warm upper mantle. At wavelengths of 3000–6000 km the depth and geoid observations are not sensitive to, and thus do not require, a deeper source for superswells. Even including longer wavelengths, cross sections of seismic tomography sliced through the South Pacific Superswell also do not show any direct connection between the hot material in the upper mantle beneath the South Pacific and warm lower mantle (Figure 26). In fact, the seismic velocity structures below 1000 km for the Darwin Rise and the Superswell are rather similar, suggesting that the difference between the active and the fossil superswell is in the upper mantle.

Although this modeling exercise considers only wavelengths between 3000 and 6000 km, *Cazenave and Thoraval* [1994] reached a very similar conclusion based on global correlations of seismic tomography, geoid, and topography at spherical harmonic degree 6 only (wavelength ≈ 7000 km). They determined that the Superswell is an upper mantle phenomenon caused by dynamic upwelling of hot material in a low-viscosity zone confined to the upper 450 km of the mantle. On the basis of the absence of deeper roots to the low-velocity material, they speculated that the plumes of French Polynesia might even originate within the transition zone rather than at the core-mantle boundary.

5.2. Thermal Modeling

We can test whether the results from dynamic modeling are consistent with the other geophysical observations from French Polynesia with one-dimensional modeling of the effect of the thermal anomalies in the asthenosphere on the lithosphere (Figure 27). The parameters in the model are chosen to simulate what might have been the thermal history for 70 Ma seafloor presently located in the vicinity of the Society Islands. Thirty

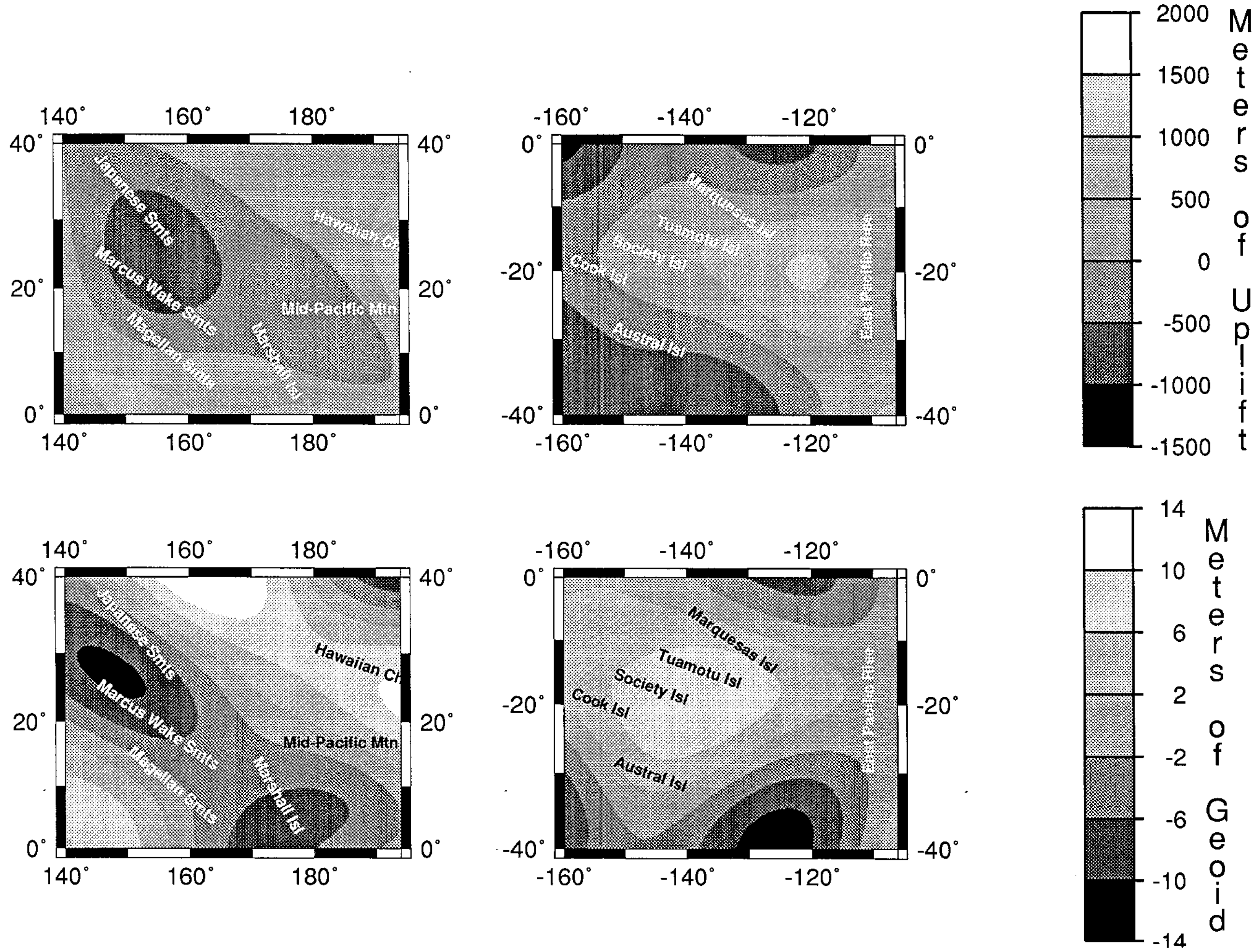

Figure 24. Predicted dynamic topography and geoid as in Figure 22, but assuming viscosity model MODSH.

million years ago, about the time anomalous volcanism began in this region on the basis of the radiometric dates of the oldest volcanoes, we assume that the thermal structure of normal lithosphere (40 Ma; dotted line) was perturbed by the arrival of a "pillow" of hot material at the upper mantle beneath the plate. The hot material was 30°C warmer than normal mantle, consistent with the inferred temperature from seismic tomography, and was allowed to penetrate only to 60-km depth (40 Ma; solid line), consistent with studies of hotspot penetration beneath midplate swells. At the present time, 30 million years later, the perturbed lithosphere (70 Ma; solid line) is warmer than normal lithosphere (70 Ma; dashed line) both on account of the initial perturbation at 40 Ma and on account of maintaining higher temperature in the asthenosphere for the ensuing 30 million years. However, the thickness of the elastic plate calculated from the depth to the 300°–600°C isotherm is still 16–33 km, consistent with the observed value of 23 ± 2 km [*Filmer et al.*, 1993], and is only 1–2 km less than the value for normal lithosphere of the same age. Similarly, the computed heat flow for this model is 48 mW m^{-2}, well within the scatter of observed values and not resolvably different from the 45 mW m^{-2} value expected for normal lithosphere. The contribution to the depth from this thermal perturbation is ~300 m. When the 750-m sublithospheric contribution from dynamic uplift (Figure 25) is added to this, we obtain the entire depth anomaly for the Superswell. These thermal anomalies have no geoid signature (kernels are zero near the surface), and the entire geoid signal is still supplied from convection beneath the plate.

The last curves in Figure 26 investigate how the old-age thermal structure of this same lithospheric section would evolve when it reaches the age of the Darwin Rise. Assuming that the plate drifts off the region of hot mantle, some thermal anomalies in the lithosphere still linger after another 50 million years (120 Ma; solid line), but the magnitude is not large because heat actually flows from the lithosphere back into the asthenosphere once the plate drifts over normal mantle of the North Pacific. In comparison with normal lithosphere of the same age (120 Ma; solid line), the predicted anomalies in depth (162 m), elastic plate thickness (2 km), and heat flow (2 mW m^{-2}) could not be resolved with current observations.

5.3. Origin of Superswells

Several researchers have suggested that superswells are dynamic phenomena. However, there are at least three different versions of the story:

1. Together, the Darwin Rise and French Polynesia represent one large superswell in the central and western Pacific caused by present-day convection patterns in the mantle [*Davies and Pribac*, 1993]. According to this explanation, the convection responsible for the South Pacific Superswell encompasses the entire western and south central Pacific.

2. The Darwin Rise and the Superswell were caused by two separate pulses of volcanism and upwelling in the mantle beneath French Polynesia, with the initiation of the two pulses separated by ~80 Myr in time [*McNutt and Judge*, 1990; *McNutt et al.*, 1990]. According to this model, the convection would be intermittent and confined to the south central Pacific.

3. The volcanism of the Darwin Rise was formed by a superplume beginning at ~120 Ma; the superswell is but the last gasp of that event 120 Myr later [*Larson*, 1991a, b]. This model also confines the convection to the south central Pacific but involves one sustained but waning event.

Davies and Pribac [1993] base their argument that the Darwin Rise and the Superswell are part of one large, dynamic feature on the fact that both regions have present-day depth anomalies relative to the half-space cooling model for the lithosphere. They are certainly justified in questioning previous work that has concluded that no depth anomaly exists at present in the area of the Darwin Rise [*McNutt et al.*, 1990; *Stein and Abbott*, 1991] in that those studies used as the depth reference plate models that had been originally calibrated using data from this area of the Pacific. *Davies and Pribac* [1993] attribute a portion of the large-scale shoaling of the central and western Pacific to convective flow in the lower mantle, which would be apparent only at wavelengths longer than the 3000- to 6000-km waveband considered here. This explanation is unnecessary for the Superswell region, where thermal anomalies in the uppermost mantle are quite sufficient to produce the entire depth anomaly, but there is no evidence for any upper mantle thermal source of uplift in the western Pacific (see *Phipps Morgan and Smith* [1992] for a nonthermal explanation). At an age of 150 Ma the Darwin Rise is 800 m shallower than the prediction from the half-space cooling curve. If a layer of mantle rock 800 m thick at degree 6 were supported by low-density material below 1000-km depth on a spherical Earth, one would expect a geoid high of 70 m over the western Pacific, although the result is dependent on the mantle model chosen. The western Pacific does have a geoid high of ~30–40 m, which might be evidence for some dynamic support of the seafloor. However, the volcanoes of the Darwin Rise have been extinct for tens of millions of years. Therefore while *Davies and Pribac*'s [1993] suggestion may have some merit for explaining the lack of half-space cooling

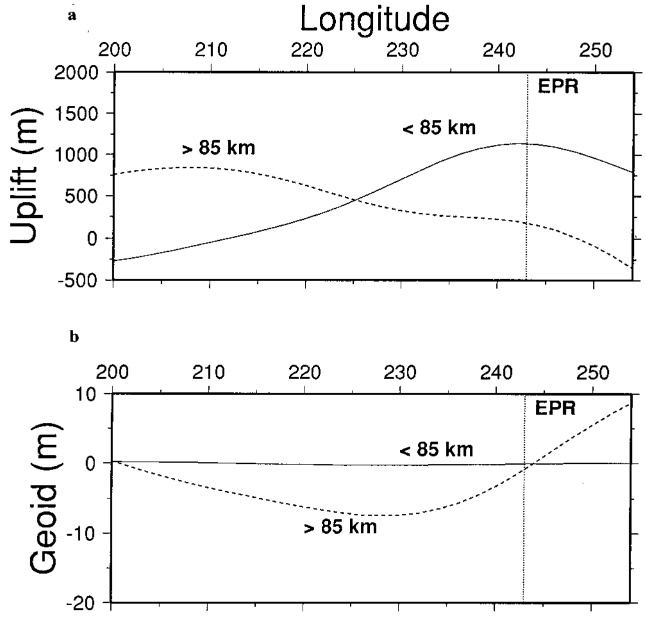

Figure 25. Cross sections along latitude 20°S of (a) uplift and (b) geoid across the South Pacific Superswell. The dashed line shows the asthenospheric component of the depth and geoid anomalies produced by density anomalies below 85 km depth, and the solid curve is the lithospheric component of the anomalies from depths of <85 km. Model HC was used to produce these predicted signals.

in the western Pacific, this is not the explanation for the Superswell. The shoaling of the Superswell is produced in the upper mantle, and it is the upper mantle source that provides its most distinctive feature: enhanced volcanism.

The fact that the volume of volcanism in the Darwin Rise approximately equals that of the Superswell is one of the strongest suggestions in favor of *McNutt and Judge*'s [1990] suggestion that the Darwin Rise and the Superswell are separate pulses of volcanism in the region of French Polynesia. However, *Larson*'s [1991a, b] superplume hypothesis includes eruption of Ontong Java and Manihiki plateaus, as well as other non-Pacific volcanic features in the same age range as the Darwin Rise but more diffuse geographically. Therefore the Superswell may be a modern-day analogue to the Darwin Rise, the latter of which occurred within the temporal context of a more global volcanic event, while the former did not. In this scenario it is only the regional event in which radiogenically enriched material convectively upwells beneath French Polynesia that is intermittent. Volcanism on the scale that created the great Pacific plateaus is not occurring today.

At present, the geophysical observations from the volcanically active Superswell can be simply explained as the result of a "pillow" of hot material in the upper mantle in the South Pacific that provides a melt source for volcanism that leaks nearly pervasively through the overlying plate (Figure 28). At the resolution of present

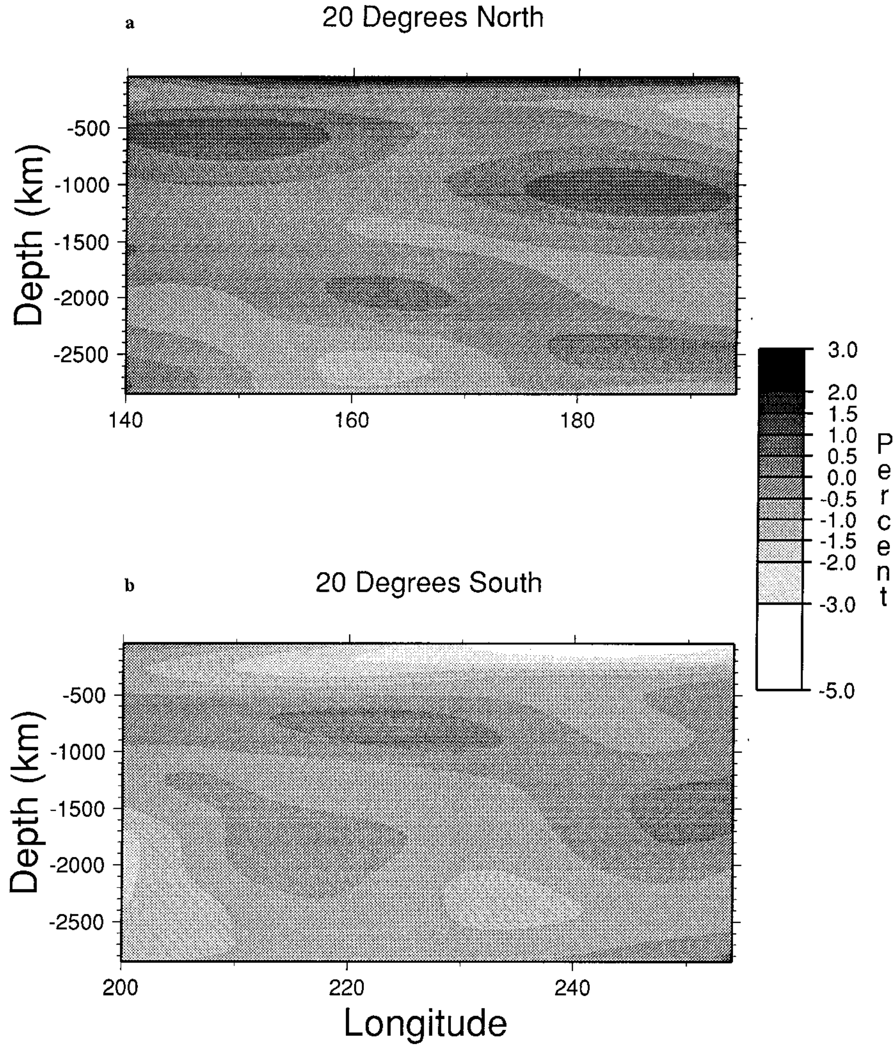

Figure 26. Cuts through the mantle from the surface to the core-mantle boundary of seismic velocity anomalies along latitude (a) 20°N (Darwin Rise) and (b) 20°S (South Pacific Superswell). Shear-wave velocity anomalies are from the aspherical model of *Su* [1992], retaining wavelengths from 13,000 to 3000 km.

seismic tomography this hot material is not presently fed by upwelling from the lower mantle, and in that sense, superswell-type volcanism is distinct from plume-type volcanism. The hot material in the upper mantle may be left over from an upwelling event from some deeper thermal boundary layer (transition zone or core-mantle boundary) in the past. On the basis of the dimensions (50° × 30° × 500 km) of the hot layer in the upper mantle and its estimated temperature anomaly from the reduction in shear wave velocity (30°C), the upwelling event that created the superswell transported about 1.2×10^{27} J of energy to the uppermost mantle, an amount equivalent to Earth's total heat flux over a period of 1 million years. By comparison, if this heat were suddenly liberated in the form of basaltic volcanism, it would create the equivalent of three Ontong Java plateaus, each with a volume of 1 million cubic kilometers [*Larson*, 1991b]. Thus the formation of a superswell transports a globally significant amount of mass and energy to the asthenosphere.

6. CONCLUSIONS

Volcanism in the present-day South Pacific Superswell, and in its Cretaceous predecessor, the Darwin Rise, is distinct from other types of volcanic activity on Earth in that it is not associated with plate separation or convergence, nor does it involve a few plumes from the deep mantle that leave isolated chains of volcanoes that age in the direction of absolute plate motion. This newly recognized type of volcanism is produced by a layer of hot, low-viscosity upper mantle beneath the Pacific plate in French Polynesia that is the melt source for volcanic activity on all scales. This layer with low degrees of partial melt produces slow seismic velocities in the asthenosphere above the transition zone, dynamic uplift of the plate, and a broad geoid low over French Polynesia.

The hot layer beneath French Polynesia is not today rooted in the lower mantle, and therefore its source remains somewhat obscure. It likely originated as an upwelling from somewhere else, such as a thermal

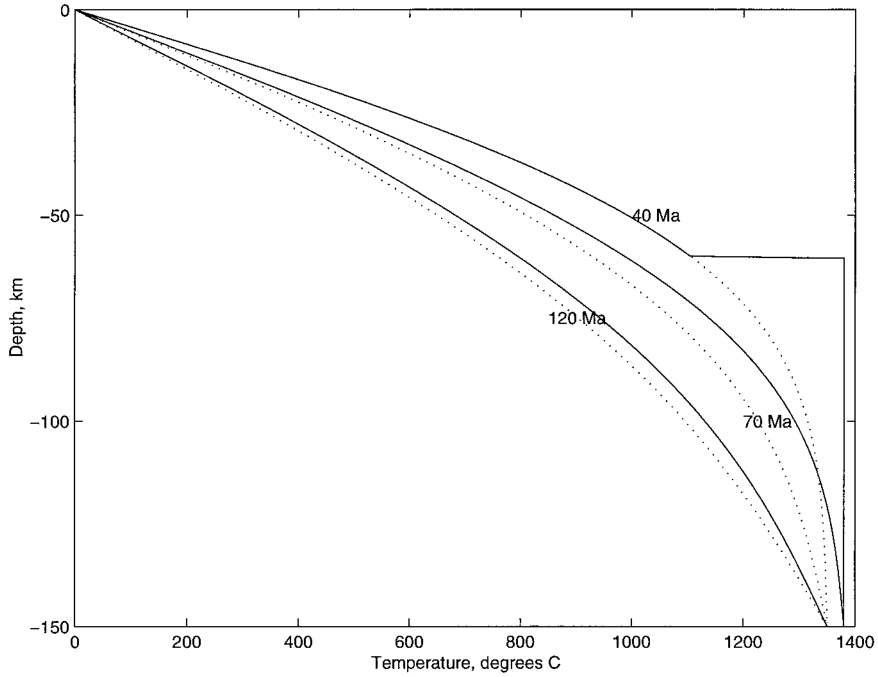

Figure 27. Results of one-dimensional thermal modeling for a 150-km-thick [*Smith and Sandwell*, 1997] lithospheric plate. Dotted lines show the thermal structure at 40, 70, and 120 Ma for normal lithosphere with an initial temperature of 1350°C. The solid lines show the perturbed thermal structure if the lithosphere is suddenly reheated by hot (1380°C) mantle to a depth of 60 km at an age of 40 Ma. The ambient mantle temperature returns to normal between 70 and 120 Ma.

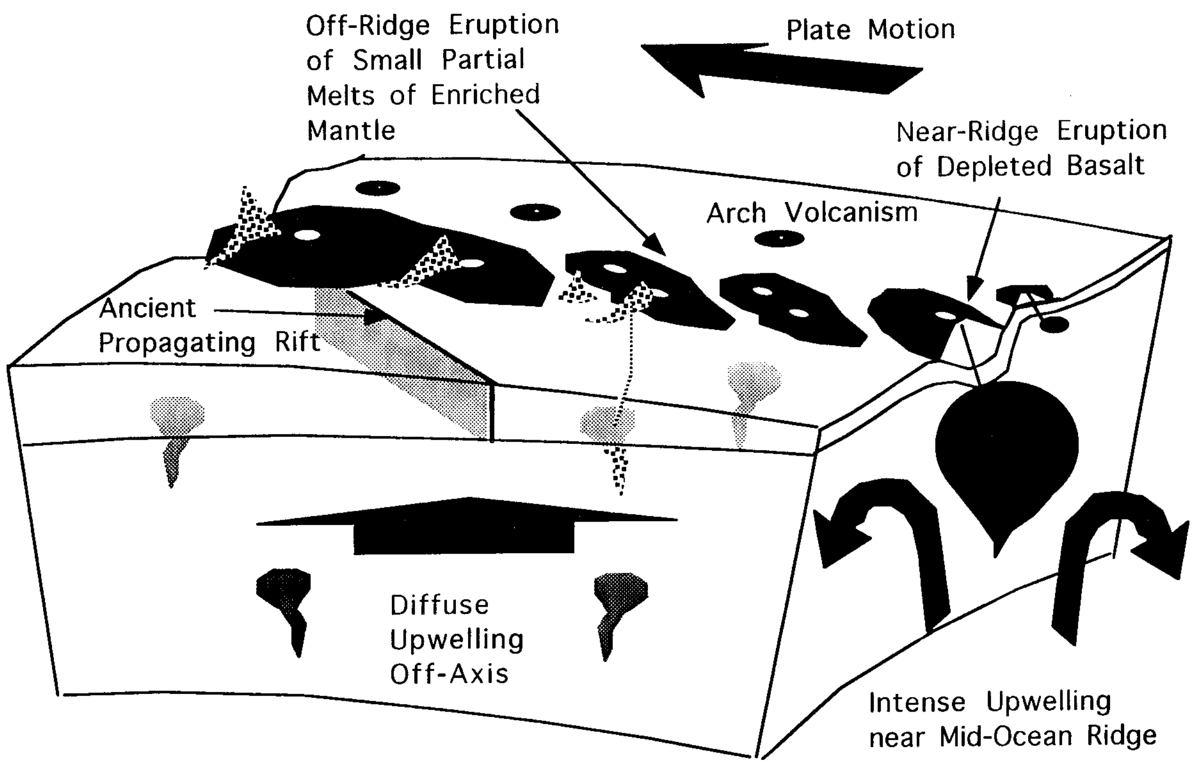

Figure 28. Diagram showing a model for superswell-type volcanism. The upper mantle beneath French Polynesia is enriched in several different easily melted components that have been reinjected into the upper mantle by earlier subduction of oceanic crust, continental crust, and sediments. Their unusual isotopic signature would be homogenized and diluted by the large degrees of partial melting that occur near the midocean ridge but preserved in the smaller off-ridge seamounts. These more exotic melts are pervasively available beneath the plate on account of diffuse upwelling but are preferentially channeled to the surface by preexisting cracks in the plate, topography on its base of the plate, and older volcanic conduits. These are generally sheared in the west-northwest direction of absolute plate motion to form lines of volcanoes, although the age progressions are often far from that predicted for a fixed mantle plume. From *McNutt et al.* [1997]; copyright 1997 Macmillan Magazines Ltd.

boundary layer in the transition zone or at the core-mantle boundary, that ponded beneath the plate, given that the radiogenic isotopes show that the volcanics are not generated from normal, depleted upper mantle, which is the source for MORB. With the slow diffusivity of heat through the lithosphere, the timing of this upwelling may even date from the major Cretaceous thermal event that created most of the major oceanic plateaus and the Superswell's predecessor, the Darwin Rise. The African superswell is probably caused by some other phenomenon; seismic data show no evidence for a regional-scale thermal source in the upper mantle for its excess elevation and intraplate volcanism.

The possibility exists that many so-called hotspots elsewhere are just miniature versions of superswell-type volcanism in that they originate as rising diapirs that melt on ascent and pond beneath the plates to form short, age-progressive volcanic sequences without further communication with the deeper mantle. These puddles of melt would leave short tracks of volcanoes in the direction of absolute plate motion, as long as the viscosity of the asthenosphere is low enough to prevent significant dragging of the asthenosphere by the lithosphere (Figure 28). As they pond beneath the plates, these melt pockets would conform to the topography on the base of the lithosphere and thus be channeled toward ridges and barricaded by transform faults and fracture zones. Long-lived plumes that consist of continuous pipes to the lower mantle, such as may be the source for long, age-progressive chains such as Hawaii, could be the exception rather than the rule.

ACKNOWLEDGMENTS. This work was funded by NSF-EAR9304621. I am indebted to Walter Smith and David Sandwell for the latest altimetry data. Martin Lee, Jerry Winterer, and Carol Stein contributed useful reviews that improved the presentation of the material.

Alan Chave thanks Jerry Winterer and another reviewer for technical reviews and Martin Lee for his cross-disciplinary review.

REFERENCES

Acton, G. D., and R. G. Gordon, Paleomagnetic tests of Pacific plate reconstructions and implications for motion between hotspots, *Science*, *263*, 1246–1254, 1994.

Anderson, D. L., Hotspots, polar wander, Mesozoic convection and the geoid, *Nature*, *297*, 391–393, 1982.

Barsczus, H. G., Les îles Australes (Polynésie Française) et la théorie des points chauds, in *Notes et Documents de Géophysique*, *Rep. 1980/27*, pp. 1–13, Inst. Fr. de Rech. Sci. pour le Dév. en Coop. (ORSTOM), Papeete, Tahiti, 1980.

Bemis, K. G., and D. K. Smith, Production of small volcanoes in the Superswell region of the South Pacific, *Earth Planet. Sci. Lett.*, *118*, 251–262, 1993.

Bonatti, E., and C. G. A. Harrison, Hot lines in the Earth's mantle, *Nature*, *263*, 402–404, 1976.

Burke, K., and J. T. Wilson, Is the African plate stationary?, *Nature*, *239*, 387–390, 1972.

Calmant, S., and A. Cazenave, The elastic thickness under the Cook-Austral and Society Islands, *Earth Planet. Sci. Lett.*, *77*, 187–202, 1986.

Calmant, S., and A. Cazenave, Anomalous elastic thickness of the oceanic lithosphere in the south-central Pacific, *Nature*, *328*, 236–238, 1987.

Caress, D. W., M. K. McNutt, R. S. Detrick, and J. C. Mutter, Seismic imaging of hotspot-related crustal underplating beneath the Marquesas Islands, *Nature*, *373*, 600–603, 1995.

Carlson, R. L., and H. P. Johnson, On modeling the thermal evolution of the oceanic upper mantle: An assessment of the cooling plate model, *J. Geophys. Res.*, *99*, 3201–3214, 1994.

Cazenave, A., and C. Thoraval, Mantle dynamics constrained by degree 6 surface topography, seismic tomography, and geoid: Inference on the origin of the South Pacific Superswell, *Earth Planet. Sci. Lett.*, *122*, 207–219, 1994.

Cazenave, A., B. Lago, K. Dominh, and K. Lambeck, On the response of the ocean lithosphere to sea-mount loads from Geos 3 satellite radar altimeter observations, *Geophys. J. R. Astron. Soc.*, *63*, 233–252, 1980.

Clague, D. A., and G. B. Dalrymple, Tectonics, geochronology, and origin of the Hawaiian-Emperor seamount chain, in *The Geology of North America*, vol. N, *The Eastern Pacific Ocean and Hawaii*, edited by E. L. Winterer, D. M. Hussong, and R. W. Decker, pp. 188–217, Geol. Soc. of Am., Boulder, Colo., 1989.

Cochran, J. R., Variations in subsidence rates along intermediate and fast spreading mid-ocean ridges, *Geophys. J. R. Astron. Soc.*, *87*, 421–454, 1986.

Crough, S. T., Thermal origin of mid-plate hot-spot swells, *Geophys. J. R. Astron. Soc.*, *55*, 451–469, 1978.

Crough, S. T., Hotspot epeirogeny, *Tectonophysics*, *61*, 321–333, 1979.

Dalrymple, G. B., R. D. Jarrard, and D. A. Clague, K-Ar ages of some volcanic rocks from the Cook and Austral Islands, *Geol. Soc. Am. Bull.*, *86*, 1463–1467, 1975.

Davies, G. F., and F. Pribac, Mesozoic seafloor subsidence and the Darwin Rise, past and present, in *The Mesozoic Pacific: Geology, Tectonics, and Volcanism*, *Geophys. Monograph. Ser.*, vol. 77, edited by M. S. Pringle et al., pp. 39–52, AGU, Washington, D. C., 1993.

Desonie, D. L., R. A. Duncan, and J. H. Natland, Temporal and geochemical variability of volcanic products of the Marquesas hot spot, *J. Geophys. Res.*, *98*, 17,649–17,665, 1993.

Detrick, R. S., and S. T. Crough, Island subsidence, hot spots, and lithospheric thinning, *J. Geophys. Res.*, *83*, 1236–1244, 1978.

Duncan, R. A., and I. MacDougall, Migration of volcanism with time in the Marquesas Islands, French Polynesia, *Earth Planet. Sci. Lett.*, *21*, 414–420, 1974.

Duncan, R. A., and I. MacDougall, Linear volcanism in French Polynesia, *J. Volcanol. Geotherm. Res.*, *1*, 197–227, 1976.

Dupuy, C., P. Vidal, H. F. Barsczus, and C. Chauvel, Origin of basalts from the Marquesas archipelago (south-central Pacific Ocean): Isotope and trace element constraints, *Earth Planet. Sci. Lett.*, *82*, 145–152, 1987.

Epp, D., Possible perturbations of hotspot traces and implications for the origin and structure of the Line Islands, *J. Geophys. Res.*, *89*, 11,273–11,286, 1984.

Filmer, P. E., M. K. McNutt, and C. J. Wolfe, Elastic thickness of the lithosphere in the Marquesas and Society Islands, *J. Geophys. Res.*, *98*, 19,565–19,577, 1993.

Filmer, P. E., M. K. McNutt, H. Webb, and D. Dixon, Volcanism and archipelagic aprons in the Marquesas and Hawaiian Islands, *Mar. Geophys. Res.*, *16*, 385–406, 1994.

Fischer, K. M., M. K. McNutt, and L. Shure, Thermal and mechanical constraints on the lithosphere beneath the Marquesas swell, *Nature*, *322*, 733–736, 1986.

Forsyth, D. W., L. M. Dorman, J. Phipps Morgan, and Y. Shen, Anisotropy and lateral variations in shear wave velocity from propagation of Rayleigh waves across the MELT array (abstract), *Eos Trans. AGU*, *77*(46), Fall Meet. Suppl., F652–F653, 1996.

Goodwillie, A. M., Short-wavelength gravity lineations and unusual flexure results at the Puka volcanic ridge system, *Earth Planet. Sci. Lett.*, *136*, 297–314, 1995.

Goodwillie, A. M., and B. Parsons, Placing bounds on lithospheric deformation in the central Pacific Ocean, *Earth Planet. Sci. Lett.*, *111*, 123–139, 1992.

Goodwillie, A. M., and A. B. Watts, An altimetric and bathymetric study of elastic thickness of the central Pacific Ocean, *Earth Planet. Sci. Lett.*, *118*, 311–326, 1993.

Hager, B. H., and R. W. Clayton, Constraints on the structure of mantle convection using seismic observations, flow models, and the geoid, in *Mantle Convection*, edited by W. R. Peltier, pp. 657–763, Gordon and Breach, Newark, N. J., 1989.

Haggerty, J. A., I. Premoli Silva, F. Rack, and the Leg 144 Scientific Party, *Proceedings of the Ocean Drilling Program; Initial Reports*, *144*, Ocean Drill. Program, College Station, Tex., 1993.

Harrison, C. G. A., K. J. Miskell, G. W. Brass, E. S. Saltzman, and J. L. Sloan, Continental hypsography, *Tectonics*, *2*, 357–377, 1983.

Hart, S. R., A large-scale isotope anomaly in the southern hemisphere mantle, *Nature*, *309*, 753–757, 1984.

Heezen, B. C., J. L. Matthews, R. Catalano, J. Natland, A. Coogan, M. Tharp, and M. Rawson, Western Pacific guyots, *Initial Rep. Deep Sea Drill. Proj.*, *20*, 653–702, 1973.

Henderson, L., Motion of the Pacific plate relative to the hotspots since the Jurassic and models of the oceanic plateaus of the Farallon plate, Ph.D. thesis, Northwestern Univ., Evanston, Ill., 1985.

Ito, G., M. McNutt, and R. L. Gibson, Crustal structure of the Tuamotu Plateau, 15°S, and implications for its origin, *J. Geophys. Res.*, *100*, 8097–8114, 1995.

Jordahl, K., M. K. McNutt, H. W. Webb, and S. E. Kruse, Why there are no earthquakes on the Marquesas Fracture Zone, *J. Geophys. Res.*, *100*, 24,431–24,447, 1995.

Jordan, T. H., Mineralogies, densities, and seismic velocities of garnet lherzolites and their geophysical implications, in *The Mantle Sample: Inclusions in Kimberlites and Other Volcanics*, edited by F. R. Boyd and H. O. A. Meyer, pp. 1–14, AGU, Washington, D. C., 1979.

King, S. D., and G. Masters, An inversion for radial viscosity structure using seismic tomography, *Geophys. Res. Lett.*, *19*, 1551–1554, 1992.

Kruse, S. E., Magnetic lineations on the flanks of the Marquesas swell: Implications for the age of the seafloor, *Geophys. Res. Lett.*, *15*, 573–576, 1988.

Larson, R. L., Late Jurrasic and early Cretaceous evolution of the western central Pacific Ocean, *J. Geomagn. Geoelectr.*, *28*, 219–236, 1976.

Larson, R. L., Latest pulse of Earth: Evidence for a mid-Cretaceous superplume, *Geology*, *19*, 547–550, 1991a.

Larson, R. L., Geological consequences of superplumes, *Geology*, *19*, 963–966, 1991b.

Larson, R. L., S. M. Smith, and C. G. Chase, Magnetic lineations of early Cretaceous age in the western equatorial Pacific Ocean, *Earth Planet. Sci. Lett.*, *15*, 315–319, 1972.

Larson, R. L., E. Erba, M. Nakanishi, E. D. Bergersen, and J. M. Lincoln, Stratigraphic, vertical subsidence, and paleolatitude histories of leg 144 guyots, *Proc. Ocean Drill. Program: Sci. Results*, *144*, 915–934, 1995.

Levitt, D. A., and D. T. Sandwell, Modal depth anomalies from multibeam bathymetry: Is there a South Pacific superswell?, *Earth Planet. Sci. Lett.*, *139*, 1–16, 1996.

Mammerickx, J., The Foundation Seamounts: Tectonic setting of a newly discovered seamount chain in the South Pacific, *Earth Planet. Sci. Lett.*, *113*, 293–306, 1992.

Marty, J. C., and A. Cazenave, Regional variations in subsidence rate of oceanic plates: A global analysis, *Earth Planet. Sci. Lett.*, *94*, 301–315, 1989.

McNutt, M. K., Temperature beneath midplate swells: The inverse problem, in *Seamounts, Islands, and Atolls*, *Geophys. Monogr. Ser.*, vol. 43, edited by B. H. Keating et al., pp. 123–132, AGU, Washington, D. C., 1987.

McNutt, M. K., and K. M. Fischer, The South Pacific superswell, in *Seamounts, Islands, and Atolls*, *Geophys. Monogr. Ser.*, vol. 43, edited by B. H. Keating et al., pp. 25–34, AGU, Washington, D. C., 1987.

McNutt, M. K., and A. V. Judge, The Superswell and mantle dynamics beneath the South Pacific, *Science*, *248*, 969–975, 1990.

McNutt, M. K., and H. W. Menard, Lithospheric flexure and uplifted atolls, *J. Geophys. Res.*, *83*, 1206–1212, 1978.

McNutt, M. K., and L. Shure, Estimating the compensation depth of the Hawaiian swell with linear filters, *J. Geophys. Res.*, *91*, 13,915–13,923, 1986.

McNutt, M. K., K. M. Fischer, S. Kruse, and J. Natland, The origin of the Marquesas fracture zone ridge and its implication for the nature of hot spots, *Earth Planet. Sci. Lett.*, *91*, 381–393, 1989.

McNutt, M. K., E. L. Winterer, W. W. Sager, J. H. Natland, and G. Ito, The Darwin Rise: A Cretaceous superswell?, *Geophys. Res. Lett.*, *17*, 1101–1104, 1990.

McNutt, M. K., L. Sichoix, and A. Bonneville, Modal depths from shipboard bathymetry: There IS a South Pacific Superswell, *Geophys. Res. Lett.*, *23*, 3397–3400, 1996.

McNutt, M. K., D. W. Caress, J. Reynolds, K. A. Jordahl, and R. A. Duncan, Failure of plume theory to explain midplate volcanism in the southern Austral Islands, *Nature*, *389*, 479–482, 1997.

Menard, H. W., *Marine Geology of the Pacific*, 271 pp., McGraw-Hill, New York, 1964.

Menard, H. W., Darwin reprise, *J. Geophys. Res.*, *89*, 9960–9968, 1984.

Molnar, P., and J. M. Stock, Relative motions of hotspots in the Pacific, Atlantic and Indian Oceans since late Cretaceous time, *Nature*, *327*, 587–591, 1987.

Morgan, W. J., Convection plumes in the lower mantle, *Nature*, *230*, 42–43, 1971.

Mueller, R. D., W. R. Roest, J.-Y. Royer, L. M. Gahagan, and J. G. Sclater, A digital age map of the ocean floor, *SIO Ref. Ser. 93-30*, Scripps Inst. of Oceanogr., La Jolla, Calif., 1993.

Nishimura, C. E., and D. W. Forsyth, Anomalous Love-wave phase velocities in the Pacific: Sequential pure-path and spherical harmonic inversion, *Geophys. J. R. Astron. Soc.*, *81*, 389–407, 1985.

Norris, R. A., and R. H. Johnson, Submarine volcanic eruptions recently located in the Pacific by SOFAR hydrophones, *J. Geophys. Res.*, *74*, 650–664, 1969.

Nyblade, A. A., and S. W. Robinson, The African superswell, *Geophys. Res. Lett.*, *21*, 765–768, 1994.

Nyblade, A. A., K. S. Vogfjord, and C. A. Langston, *P*-wave velocity of Proterozoic upper mantle beneath central and southern Africa, *J. Geophys. Res.*, *101*, 11,159–11,172, 1996.

Palacz, Z., and A. D. Saunders, Coupled trace element and isotope enrichment in the Cook-Austral-Samoa Islands, southwest Pacific, *Earth Planet. Sci. Lett.*, *79*, 270–280, 1986.

Parsons, B., and J. G. Sclater, An analysis of the variation of the ocean floor bathymetry and heat flow with age, *J. Geophys. Res.*, *82*, 803–827, 1977.

Phipps Morgan, J., and W. Smith, Flattening of the seafloor depth-age curve as a response to asthenospheric flow, *Nature*, *359*, 524–527, 1992.

Phipps Morgan, J., W. J. Morgan, and E. Price, Hot spot melting generates both hot spot volcanism and a hot spot swell?, *J. Geophys. Res.*, *100*, 8045–8062, 1995.

Robinson, E. M., B. Parsons, and S. Daly, The effect of a shallow low-viscosity zone on the apparent compensation of midplate swells, *Earth Planet. Sci. Lett.*, *82*, 335–348, 1987.

Sager, W. W., E. L. Winterer, J. V. Firth, and the Leg 144 Scientific Party, *Proceedings of the Ocean Drilling Program; Initial Reports*, *143*, Ocean Drill. Program, College Station, Tex., 1993.

Sandwell, D. T., E. L. Winterer, J. Mammerickx, R. A. Duncan, M. A. Lynch, D. A. Levitt, and C. L. Johnson, Evidence for diffuse extension of the Pacific plate from the Pukapuka Ridges and crossgrain gravity lineations, *J. Geophys. Res.*, *100*, 15,087–15,099, 1995.

Schlanger, S. O., and I. Premoli Silva, Tectonic, volcanic, and paleogeographic inplications of redeposited reef faunas of Late Cretaceous and Tertiary age from the Nauru Basin and the Line Islands, *Initial Rep. Deep Sea Drill. Proj.*, *61*, 817–828, 1981.

Schlanger, S. O., M. O. Garcia, B. H. Keating, J. J. Naughton, W. W. Sager, J. A. Haggerty, J. A. Philpotts, and R. A. Duncan, Geology and geochronology of the Line Islands, *J. Geophys. Res.*, *89*, 11,261–11,272, 1984.

Shen, Y., D. W. Forsyth, D. S. Scheirer, and K. C. Macdonald, Two forms of volcanism: Implications for mantle flow and off-axis crustal production on the west flank of the southern East Pacific Rise, *J. Geophys. Res.*, *98*, 17,875–17,889, 1993.

Sichoix, L., and A. Bonneville, Prediction of bathymetry in French Polynesia constrained by shipboard data, *Geophys. Res. Lett.*, *23*, 2469–2472, 1996.

Sleep, N. H., Hotspots and mantle plumes: Some phenomenology, *J. Geophys. Res.*, *95*, 6715–6736, 1990.

Smith, D. K., and T. H. Jordan, Seamount statistics in the Pacific Ocean, *J. Geophys. Res.*, *93*, 2899–2918, 1988.

Smith, W. H. F., On the accuracy of digital bathymetric data, *J. Geophys. Res.*, *98*, 9591–9604, 1993.

Smith, W. H. F., and D. T. Sandwell, Global seafloor topography from satellite altimetry and ship depth soundings, *Science*, *277*, 1956–1962, 1997.

Smith, W. H. F., H. Staudigel, A. B. Watts, and M. S. Pringle, The Magellan Seamounts: Early Cretaceous record of the South Pacific isotopic and thermal anomaly, *J. Geophys. Res.*, *94*, 10,501–10,523, 1989.

Staudigel, H., K.-H. Park, M. Pringle, J. L. Rubenstone, W. H. F. Smith, and A. Zindler, The longevity of the South Pacific isotopic and thermal anomaly, *Earth Planet. Sci. Lett.*, *102*, 24–44, 1991.

Stein, C. A., and D. H. Abbott, Heat flow constraints on the South Pacific superswell, *J. Geophys. Res.*, *96*, 16,083–16,100, 1991.

Stein, C. A., and S. Stein, A model for the global variation in oceanic depth and heat flow with lithospheric age, *Nature*, *359*, 123–129, 1992.

Stein, C. A., and S. Stein, Constraints on hydrothermal heat flux through the oceanic lithosphere from global heat flow, *J. Geophys. Res.*, *99*, 3081–3095, 1994.

Steinberger, B. M., Motion of hotspots and changes of the Earth's rotation axis caused by a convecting mantle, Ph.D. dissertation, Harvard Univ., Cambridge, Mass., 1996.

Stouffers, P., Active Pitcairn hotspot found, *Mar. Geol.*, *95*, 51–55, 1990.

Su, W.-J., The three-dimensional shear-wave velocity structure of the Earth's mantle, Ph.D. thesis, Harvard Univ., Cambridge, Mass., 1992.

Talandier, J., and E. Okal, New surveys of Macdonald Seamount, south central Pacific, following volcanoseismic activity, 1977–1983, *Geophys. Res. Lett.*, *11*, 813–816, 1984a.

Talandier, J., and E. Okal, The volcanoseismic swarms of 1981–1983 in the Tahiti-Mehetia area, French Polynesia, *J. Geophys. Res.*, *89*, 11,216–11,234, 1984b.

Talandier, J., and E. Okal, Seismic detection of underwater volcanism: The example of French Polynesia, *Pure Appl. Geophys.*, *125*, 919–950, 1987.

Tarduno, J. A., and J. Gee, Large-scale motion between Pacific and Atlantic hotspots, *Nature*, *378*, 477–480, 1995.

Turner, D. L., and R. D. Jarrard, K-Ar dating of the Cook-Austral Island chain: A test of the hot spot hypothesis, *J. Volcanol. Geotherm. Res.*, *12*, 187–220, 1982.

Van Wykhouse, R., SYNBAPS, *Tech. Rep. TR-233*, Natl. Oceanogr. Off., Washington, D. C., 1973.

Vidal, P., C. Chauvel, and R. Brousse, Large mantle heterogeneity beneath French Polynesia, *Nature*, *307*, 536–538, 1984.

Watts, A. B., J. H. Bodine, and N. R. Ribe, Observations of flexure and the geological evolution of the Pacific basin, *Nature*, *283*, 532–537, 1980.

Wessel, P., and W. H. F. Smith, Free software helps map and display data, *Eos Trans. AGU*, *72*, 441, 445–446, 1991.

White, W. M., Sources of oceanic basalts: Radiogenic isotope evidence, *Geology*, *13*, 115–118, 1985.

Wilson, J. T., Evidence from islands on the spreading of the ocean floor, *Nature*, *197*, 536–538, 1963.

Winterer, E. L., J. H. Natland, R. J. Van Waasbergen, R. A. Duncan, M. K. McNutt, C. J. Wolfe, I. Premoli Silva, W. W. Sager, and W. V. Sliter, Cretaceous guyots in the northwest Pacific: An overview of their geology and geophysics, in *The Mesozoic Pacific: Geology, Tectonics, and Volcanism*, *Geophys. Monogr. Ser.*, vol. 77, edited by M. S. Pringle et al., pp. 307–334, AGU, Washington, D. C., 1993.

Wolfe, C. J., and M. K. McNutt, Compensation of Cretaceous seamounts of the Darwin Rise, northwest Pacific Ocean, *J. Geophys. Res.*, *96*, 2363–2374, 1991.

Wolfe, C. J., M. K. McNutt, and R. S. Detrick, The Marquesas archipelagic apron: Seismic stratigraphy and implications for volcano growth, mass wasting, and crustal underplating, *J. Geophys. Res.*, *99*, 13,591–13,608, 1994.

Wolfe, C. J., I. T. Bjarnason, J. C. VanDecar, and S. C. Solomon, Seismic structure of the Iceland mantle plume, *Nature*, *385*, 245–247, 1997.

Zhou, H., A high-resolution P wave model for the top 1200 km of the mantle, *J. Geophys. Res.*, *101*, 27,791–27,810, 1996.

Zindler, A., and S. Hart, Chemical geodynamics, *Annu. Rev. Earth Planet. Sci.*, *14*, 493–571, 1986.

M. K. McNutt, Monterey Bay Aquarium Research Institute, P.O. Box 628, 7700 Sandholdt Road, Moss Landing, CA 95039-0628. (e-mail: marcia@mbari.org)